

**ANGLE OF INTERNAL FRICTION AND COHESION OF
CONSOLIDATED GROUND MARIGOLD PETALS
AS A FUNCTION OF PARTICLE SIZE,
MOISTURE CONTENT, AND FLOW
ENHANCER**

By

YU ZOU

Bachelor of Science

South China University of Technology

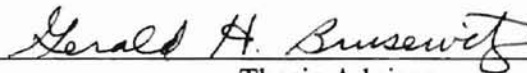
Guangzhou, China

1993

**Submitted to the Faculty of the
Graduate College of the
Oklahoma State University
in partial fulfillment of
the requirements for
the Degree of
MASTER OF SCIENCE
July, 2000**

**ANGLE OF INTERNAL FRICTION AND COHESION OF
CONSOLIDATED GROUND MARIGOLD PETALS
AS A FUNCTION OF PARTICLE SIZE,
MOISTURE CONTENT, AND FLOW
ENHANCER**

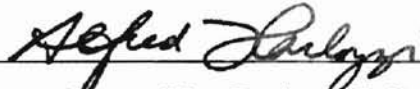
Thesis Approved:



Thesis Advisor







Dean of the Graduate College

ACKNOWLEDGEMENTS

I would like to express my most appreciation to Dr. Gerald H. Brusewitz, my advisor, who provided me with numerous good advice and support during the research, spent a great deal of hours revising the technical and grammar errors and improving the accuracy and style of this thesis. I can not express my gratitude in words to his helpful guidance through my study in Oklahoma State University. His knowledge, kindness and patience impressed me a lot. I am very grateful to Mr. Bruno Cateni, who gave me a lot of support on the experiment setup. I would like to thank the members of my graduate committee, Dr. Danielle Bellmer, and Dr. Marvin Stone, for their suggestions during the research.

Thanks to Mr. Tom Underwood, who helped me on the preparation of the experiment and tutored me in English in his free time. I would like to thank the Biosystems and Agricultural Engineering Department that gave me the financial support on this research.

Specially, I thank my parents for their love and guidance throughout my life.

TABLE OF CONTENTS

Chapter	Page
I. INTRODUCTION.....	1
II. LITERATURE REVIEW.....	4
Flowability Theory.....	4
Variables for Flow Properties.....	4
Yield Locus.....	4
Flowability Measurement.....	5
Overview of Methods.....	5
Direct Shear Cell Method.....	6
Jenike Shear Cell Method.....	7
Measuring Flowability by the Angle of Repose.....	7
Other Methods.....	8
Effect of Properties on Flowability.....	10
Effect of Particle Size.....	10
Effect of Moisture Content.....	11
Effect of Flow Enhancer.....	13
III. MATERIALS, EQUIPMENT, AND METHODS.....	16
Test Materials.....	16
Physical Properties.....	16
Particle Size.....	16
Bulk Density.....	17
Moisture Content.....	17
Description of the Shear Testing System.....	18
Experimental Methods.....	20
Calibration of the Shear Testing System.....	22
Data Analysis.....	23
IV. RESULTS AND DISCUSSION.....	24
Effect of Particle Size.....	29
Effect of Moisture Content.....	33
Effect of Flow Enhancer.....	36

Chapter	Page
Main Effects.....	39
Effect of Interactions.....	42
Regression Analysis.....	46
Test at Different Mass.....	47
Further Discussion.....	48
V. SUMMARY AND CONCLUSIONS.....	50
Summary.....	50
Conclusions.....	51
VI. RECOMMENDATIONS FOR FUTURE STUDY.....	52
BIBLIOGRAPHY.....	53
APPENDIX.....	60
A.1 Regression Analysis	60
A.2 Particle Size Analysis.....	67

LIST OF TABLES

Table	Page
3.1 Moisture Content, Dry Basis, of Ground Marigold Petals.....	18
3.2 Actual Weight of Ground Marigold Petals.....	20
3.3 Filling, Tapping and Consolidation of the Sample.....	21
4.1 Normal Stresses and Corresponding Shear Stresses for Each Treatment.....	26
4.2 Angles of Internal Friction and Cohesion Coefficients for Each Treatment.....	28
4.3 Means and Standard Deviations of Angle of Internal Friction and Cohesion Coefficients.....	29

LIST OF FIGURES

Figure	Page
3.1 Schematic Diagram of the Direct Shear Cell.....	19
4.1 A Typical Shear Force Vs. Time Graph.....	24
4.2 A Typical Yield Locus for Shear Stress vs. Normal Stress.....	27
4.3 The Effect of Particle Size on the Angle of Internal Friction.....	31
4.4 The Effect of Particle Size on Cohesion.....	32
4.5 The Effect of Moisture Content(RH in Conditioning Chamber) on the Angle of Internal Friction.....	34
4.6 The Effect of Moisture Content(RH in Conditioning Chamber) on Cohesion.....	35
4.7 The Effect of Flow Enhancer on the Angle of Internal Friction.....	37
4.8 The Effect of Flow Enhancer on Cohesion.....	38
4.9 Main Effect Plot for Angle of Internal Friction.....	40
4.10 Main Effect Plot for Cohesion.....	41
4.11 Interaction Plot for Angle of Internal Friction.....	44
4.12 Interaction Plot for Cohesion.....	45
4.13 The Graph of Relationship between Depth And Density in Silage.....	49

CHAPTER I

INTRODUCTION

The color of the yolk is one of the most important factors in egg quality. Although color does not provide any different amount of nutrition, people prefer to buy eggs that have brighter pigmented egg yolks. The color of an egg yolk is produced by xanthophylls in the feed (Delgado, 1998). Important sources of xanthophylls are corn and marigold flowers in the poultry feed industry. Feeds with low amounts of corn usually will be supplemented with marigold flowers. Whole marigold petals are difficult to handle and thus are ground into powders. Ground marigold petals are stored in large bulk quantities in bins and moved by conveyers or gravity flow. Obviously, the better the flowability, the less likely they will cake and the easier they will flow out of the bins.

The flow properties of poultry feed are important to design and operation of storage facilities and handling equipment. The flowability of ground powders in general is described by one of four qualitative levels: very good, good, medium and bad flowability. Quantitative data are available for some food powders, but no quantitative data on the flowability of ground consolidated marigold petals were found in the literature.

The term “flowability” includes two stages: the ease or difficulty of a powder to start flowing and for it to continue to flow. When an aperture in the base of a bin is opened, powders under gravity may discharge easily or with no discharge at all. Even when powders discharge easily at the very beginning, they may stop flowing due to bin geometry or high compaction of materials inside the bin. Flowability is sometimes

considered without packing, i.e., no compaction. Hauhouot-O'Hara (1999) considered angle of repose as a parameter to describe the flow properties of unconsolidated ground marigold petals. The angle of repose is useful for calculations concerned with utilization of hopper volume. However, when powders are stored under pressure in 5-10 m high bins, angle of repose is not adequate to explain what occurs inside the mass because it does not relate to the strength of a powder subjected to the compaction stresses in storage (Svarpovsky, 1987). When powders are compacted, the flowability of powders should consider how the shear strength depends on the compacting force acting on it. In this case, wall friction coefficient, flow function, effective angle of internal friction, and angle of internal friction are suggested as parameters needed to determine the flow properties when powders are stored under pressure (Jenike, 1987), among which the angle of internal friction is considered as one of the physical properties directly affecting storage-bin wall lateral pressures (Stewart, 1968).

Flowability is affected by bin geometry and material properties. In the literature, particle size usually is related to flowability of powders. Moisture content is another important factor that may affect the angle of internal friction in different directions. Kamath (1994) found that the angle of internal friction increased with moisture content for wheat flour. Duffy (1996) found that the angle of internal friction decreased with increase in moisture content for both confectionery sugar and detergent powder. He also (1999) compared angle of internal friction of coated cottonseeds, shelled corn and soybeans and found no trend in the angle of internal friction with moisture content between 8.3% and 12.8%. Chang (1998) said that the angle of internal friction decreased at higher water activity for model food powders composed of starchy powder and proteinaceous powder. He suggested that this might be due to the reduction in the

particle's surface roughness through dissolution and lubrication. Powders may easily cake under pressure, i.e., consolidation, during packaging, storage or transportation. Adding a flow enhancer, such as aluminum silicate, calcium stearate, calcium sulfate, tricalcium phosphate, magnesium carbonate, cornstarch, diatomaceous earth, or kaolin, will increase the flowability of powders. Peleg (1973) found that angle of internal friction decreased with the addition of calcium stearate while aluminium silicate slightly increased it. Other factors related to flowability are nature of the powder, its composition, size distribution, bulk density, packing of particles, temperature, and consolidation time (Pilpel, 1970).

The objective of this research was to determine the flow properties of consolidated ground marigold petals and how they were affected by particle size, moisture content and addition of flow enhancer. The method used for measuring the flowability was shear testing with a direct shear cell. Shear tests at three normal loads provided the data to compute the angle of internal friction and cohesion, the parameters needed to compare the flow properties of consolidated ground marigold petals with different treatments.

CHAPTER II

LITERATURE REVIEW

Flowability Theory

Variables for flow properties

The theory of flowability of powder was first developed at the University of Utah by Jenike in 1964. Test equipment and methods have been developed and refined to measure relevant flow properties. Six primary variables were used to evaluate flow properties: wall friction coefficient, flow function, effective angle of internal friction, angle of internal friction, bulk density, and permeability. Most of them are measured on a direct shear tester (Jenike and Carson, 1987).

Yield locus

The principle of operation for the direct shear cell, the Jenike shear cell and the ring rotational split-level shear cell is the same. The yield locus for these testers is: $\tau = \sigma \tan \Phi + C$ where τ is the shear stress, σ is the normal stress, Φ is the angle of internal friction, and C is cohesion. The yield locus for the triaxial cell is: $[(\sigma_1 - \sigma_2)/2] = [(\sigma_1 + \sigma_3)/2] \sin \Phi + \cos \Phi$ where σ_1 and σ_3 , respectively, are the axial (major) and lateral (minor) principal stresses (Kamath et al., 1993).

Flowability Measurement

Overview of methods

Schulze (1996a, 1996b) in reviewing 16 flowability test methods concluded that the Jenike shear test was the most accurate method. However, because correctly operating the Jenike test equipment requires extensive training and experience, the ring shear and torsional shear tests are reasonable options. The author also discussed three testing factors; the consolidation procedures, sample anisotropy, and working plane stresses, which influence flowability measurements and concluded that tests using similar consolidation stress but different consolidation procedures produced different results. Peleg (1977) surveyed flowability test methods based on Jenike shear cell, annular cells, angle of repose, angle of internal friction, tensile strength for the soup mix, the unconfined yield locus and flow function, the “Hausner Ratio” (the ratio between tap and apparent bulk densities) compressibility, and rotational viscometry for milk powder. The static angle of internal friction was affected by bulk density and therefore by the consolidation pressure for the “complex” or “irregular” powders. Kamath et al. (1993) in measuring the flow properties of wheat flour and sugar, compared the advantages and disadvantages of the Jenike shear cell, the direct shear cell, the triaxial cell, and rotational split-level shear cell (RSL). By using the direct shear cell according to ASTM standard D3080-90 (1998), one can obtain a yield locus quickly with easily reproducible results. However, the flow function cannot be determined from this tester. Using the Jenike shear cell allows one to obtain the flow function, but there is no standard procedure accepted and the test requires expertise in proper specimen preparation and achieving optimum consolidation. The flow properties determined from the four testers were similar for wheat flour and the estimated cohesion coefficients were similar for

sugar. However, the $\tan \Phi$ values from RSL shear cell were significantly different from the other three testers. A possible reason for the high estimated value of $\tan \Phi$ for sugar from the RSL shear cell was the lack of sufficient expansion space for the sugar along the shear plane in the cell.

Direct shear cell method

Tsunakawa (1982) developed a direct shear tester equipped with a press loading system to measure the flow properties of granular materials and cohesive powders. The yield locus for granular materials (glass beads, steel ball, cation exchange resin, anion exchange resin, silica sand, oil coke, crushed coal, wheat, soybean, rape seed, milo, sugar, salt, lactose agglomerate, polyester pellets, polycarbonated pellets, polystyrene beads, low-pressure polyethylene pellets, high-pressure polyethylene pellets, ethylene-vinylacetate copolymer pellets) produces a straight line of shear stress vs. normal stress. The angle of repose, angle of internal friction, and angle of wall friction for these materials used together with their physical properties (particle shape, particle size, particle density and bulk density) were listed. The yield loci for cohesive powders (magnesium oxide, calcium carbonate, calcium phosphate, fish powder, polyethylene) were convex curves. The yield loci for a range of initial consolidation stresses of 10 to 350 g/cm² were satisfactorily described by the Warren Spring equation $(\tau/C)^n = (\sigma+T)/T$. When this equation was rewritten with reduced stresses for cohesive powder, it could be expressed in terms of three dimensionless parameters which depend on the bulk density of the sample. Negi et al.(1987) determined the bulk density and internal friction properties of alfalfa and corn silages using the direct shear cell and examined the

influence of moisture content on flow properties. Moisture content in the range of 65-76% had no effect on the angle of internal friction and cohesion of silage materials.

Average values of cohesion and angle of internal friction were found to be 1kPa and 30°, respectively.

Jenike shear cell method

Kandala and Puri (1998) measured the flow properties of limestone, glass fibers, ground silica, microcrystalline cellulose and wheat flour at low consolidation loads (1-6 kPa) using the computer controlled shear cell (CCSC) as a Jenike tester (CCJT) and as a dynamic yield locus tester (DYLT). The cohesion and angle of internal friction were similar for ground silica and glass fibers. The angle of internal friction at consolidation stress of 5.2 kPa was the only flow property significantly different for microcrystalline cellulose. Four of the six flow parameters were significantly different for wheat flour. The flow parameters for all five powders were similar at a consolidation stress of 1.2 kPa, which shows that the CCSC is a useful tool to measure flow properties at low pressures.

Measuring flowability by the angle of repose

Train (1958) compared four methods - fixed funnel to produce free standing cone, fixed bed cone, tilting box, and revolving cylinder to determine the angle of repose of free flowing powders. The coefficient of static friction had a larger value than the coefficient of kinetic friction for glass balls, lead shot and silver sand. Direct comparison between methods was difficult because of differences between the mass of the powder heap. The first two methods gave results that were lower than those given by

the second two methods. Hauhouot-O'Hara et al.(1999) investigated the flowability of ground marigold petals by measuring its loose and rolling angle of repose. They found a significant effect of particle size and adding flow enhancer (TCP) but no significant effect due to moisture content.

Other Methods

Schulze (1996c) compared the ring shear tester and the Jenike shear tester, noting the advantage of the ring shear cell, and evaluated the flowability of pharmaceutical powders, limestone powder and metal powder mixed with different additives. He found that nearly the same flow function could be obtained from both testers. However, the ring shear tester overcame certain limitations of the Jenike shear tester. It allowed measurement at consolidation stresses down to about 400-500 Pa, easier to operate, and the results are less dependent on the operator's skill. Haaker et al.(1993) developed a translational shear tester to work with a constant volume sample. Different methods for testing limestone were tried, following the standard shear testing technique and the new method with constant density. The results showed no real trends. Kozler and Novosad (1989) tested the flowability of fertilizers using a quicker and simpler approach to measure the flow function. Their method consists of compacting the fertilizer with a major consolidating stress σ_1 and then determining the unconfined yield strength σ_{ce} needed to cause failure in the sample. The method utilized an empirical way by setting the height-to-diameter ratio of the compacted sample in such a manner that σ_{ce} nearly coincides with the unconfined yield strength σ_c as determined from a Jenike shear tester. The method gave a good qualitative distinction between satisfactory and unsatisfactory

results. To obtain a homogeneous bulk density, Williams et al.(1971) filled the mould stepwise by dividing the fill of material in several (3-20) increments. Ploof and Carson (1997) introduced a quality control tester to determine relative flowability of powders (such as titanium dioxide, limestone dust and water mix) by measuring the pressure at failure, and compared it to the established value for a “good” material. Materials with larger particle size typically showed less cohesive strength. Gentry et al.(1970) reviewed several types of test apparatus and methods for testing the flowability of sand. Hollenbach and Peleg (1983) compared the bulk properties, compressibility and appearance of particles of the conditioned and untreated powders (sodium chloride, soy protein and cornstarch). The conditioners used were calcium stearate, sodium silicon aluminate, silicon oxide and tricalcium phosphate. There were at least three degrees of surface affinity: complete adherence, partial adherence and no adherence. The magnitude of the change in the bulk properties was associated with the degree of surface coverage. Where surface affinity was strong, noticeable effects on bulk properties occurred at concentrations as low as 0.1 - 0.5%. Where there was little affinity, the effects were significant only at higher concentrations, i.e., 1-2%. Stainforth and Berey (1973) developed a general flowability index for powders. For “regular” powders (those that show both a constant shear index, n , and angle of static internal friction), the flowability index (ξ) is:

$$\xi = \frac{[1 - (n - 1)\sin\psi][1 - (n - 1)\sin^2\psi]}{2n\sin\psi} * 100 \quad (2.1)$$

For “irregular” powders (those that show a variable n and angle of internal friction with increasing stress, temperature or dampness), the flowability index (ξ) is:

$$\xi = \frac{[1 - (n - 1)\sin\psi][1 - \sin\psi][G - (n - 1)/G]}{2n\sin\psi(G - 1)} * 100 \quad (2.2)$$

where Ψ is static internal friction, $G^2 = 1 + n^2 \cot^2 \Delta$, and Δ is the major angle of internal friction. They present a classification table for 60 regular powders.

Effect of Properties on Flowability

Effect of particle size

Hauhouot-O' Hara et al. (1999) found that the effects of particle size on both angle of repose and rolling angle of repose were nonlinear. Particle size significantly affected the angle of repose. Larger particles had higher angles of repose. The rolling angle of repose sometimes increased or sometimes decreased with larger particle sizes, depending on moisture content and amount of flow enhancer. Ramanan et al. (1981) analyzed the flow properties of raw cement mix by a Jenike shear cell and described the effect of fines and size distribution on the flowability of powder material. There was a random variation of flow factor for sizes 10 μm , 20 μm , 30 μm , 40 μm , but for particles less than 5 μm , the plot showed a regular variation similar to the trend observed by Schonlebe (1991). The flow property was controlled by the coarse fraction unless the amount of fines was less than 16.5%. The fines controlled the flow property when the amount of fines exceeded 43.5%. Kocova and Pilpel (1972) investigated the relationship between the angle of internal friction, the particle size of powders in the range of 3-55 μm , and packing densities for lactose and calcium carbonate powders. The angle of internal friction, the specific tensile stress, the specific cohesion and the shear index of these two powders were independent of the powders' packing densities, hence they were considered "simple" powders. Kurz and Munz (1975) determined the relationship between the particle size distribution and flow properties for limestone (3.1-55 μm) powders using Jenike shear cell. The average particle size could not be used alone for

characterizing flow behavior. Markedly different flow function values existed for similar particle sizes. Free flow for narrow particle size distributions (variation coefficient $c_3 \leq 0.5$, where variation coefficient was defined as standard deviation divided by average particle size) occurred for average particle sizes greater than 8 μm . Cohesive flow behavior was also possible for particles greater than 8 μm if $c_3 \geq 0.5$. Limestone powders with narrow particle size distributions ($c_3 \leq 0.5$) were cohesionless for porosity of the bulk material ϵ of about 0.5. For cohesive powders, the values of unconfined yield pressure, effective angle of friction and porosity of the bulk material were higher than that of free flowing powders.

Effect of moisture content

Hauhouot-O' Hara et al. (1999) concluded that higher moisture content in marigold petals produced a higher but not significant angle of repose. Duffy and Puri (1996) measured the flowability parameters, cohesion and internal angle of friction using the Jenike shear cell of two particulate materials, at two moisture contents (0.3%, 3.3% for confectionery sugar and 1.4%, 4.4% for detergent powder). The internal angle of friction decreased 59 and 24% with an increase in moisture content for confectionery sugar and detergent powder, respectively. The angle of friction of confectionery sugar on stainless steel and aluminum decreased by 22% and 9%, respectively. The angle of friction of detergent powder on stainless steel and aluminum decreased by 42% and 30%, respectively. Duffy and Puri (1999) measured angles of internal friction using the Jenike shear cell at three moisture contents (8.7%, 10.8% and 12.4% for coated cottonseeds, 8.3%, 11.1% and 12.8% for shelled corn, 8.3%, 11.1% and 12.4% for soybeans). Coated cottonseeds and shelled corn had similar angles of internal friction. Soybeans had

significantly higher angles of internal friction than coated cottonseeds and shelled corn. However, soybean sheared with a distinct failure, which was not apparent for coated cottonseeds and shelled corn. The three materials exhibited no significant cohesion and no observable trend in the angle of internal friction as a function of moisture content between 8.3% and 12.8%. Kamath et al.(1994) measured the flow properties (cohesion and slope of the yield locus) of wheat flour at three different moisture contents (11.8%, 14.7% and 16.4%) using the Jenike shear tester with no time consolidation, i.e., instantaneous yield loci, over a range of loading conditions. Cohesion and yield locus slopes were similar for the three moisture contents. The flow properties of wheat flour at 11.8% moisture content and consolidation times of 12h and 24h were not significant different. Lai et al.(1985) investigated flow properties (loose bulk density, compressibility and tensile strength) of two egg powders, whole egg with corn syrup and salt (CEP) and whole egg powder (WEP). Free-flowing characteristics of both powders decreased at higher temperature. Moisture content had a significant affect on the flowability of CEP, but not WEP. Murthy and Bhattacharya (1998) determined the physical properties (size, roundness, sphericity, bulk density, angle of repose and flowability) and uniaxial compression properties (failure force, failure strain, linear strain limit, energy for failure and deformation modulus) of black pepper at moisture contents from 8 to 32%. Angle of repose increased while flowability decreased at higher moisture contents, especially above 14%. Teunou et al.(1999) compared the flowability using an annular shear cell of flour, skim-milk, tea and whey – permeate as affected by their physical properties (particle size, tapped bulk density, particle density, water sorption isotherms, and relative humidity. Bulk density was determined using an Engelsmann model A-G mechanical tapping device where the volume of a given mass of

powder was measured after 1250 taps. Particle density was measured using a Micromeritics multivolume nitrogen gas pycnometer. Skim-milk powder is a free flowing powder because of its low water content and large particle size. Whey – permeate powder is an easy flowing powder but its flow index is less than milk due to its smaller particle size. Flour is a cohesive powder due to its higher water content. Tea powder exhibits moderate flow due to its small particle sizes and low water content. Teunou and Fitzpatrick (1999) found for flour, tea and whey permeate, a decrease in flowability when relative humidity and temperature increased, except for flour where flowability increased at higher temperatures. Humidity had a strong influence on the flowability of tea and whey-permeate powders but a less significant effect on flour.

Effect of flow enhancer

Six mechanisms on how flow enhancers affect the flowability of powders were well explained by Peleg and Hollenbach (1984). Hauhouot-O' Hara et al. (1999) found that both the loose angle of repose and the rolling angle of repose of marigold petals decreased with addition of tricalcium phosphate. Adding as little as 1% TCP reduced angles of repose by 3° with larger amounts of TCP having no further effect. Irani (1959) said that there was an optimum conditioner level for each conditioner - material system, beyond which flow would not change significantly or even became poorer. Ludlow and Aukland (1990) said that powders cake because of temperature, moisture migration and particle size. Proper conditioning was the major step to prevent caking or flowability problems with sugar. They recommended that humidity be maintained at 55 to 65%, temperature at 13-18 °C and to blow dry air up through the sugar for at least 72 hours. Lai et al. (1986) studied water sorption and flow properties of whole egg powder

with and without flow conditioners. Adding flow conditioner silica and sodium silico-aluminate improved the egg powder's flowability by modifying the particle surface. Adding a flow conditioner appeared to eliminate the moisture hysteresis loop. Moisture uptake by powders with flow conditioners was greater than by those without. Irani et al.(1959) investigated the effect of eight different conditioners on the flowability of materials (cocoa, dichlorodiphenyltrichloroethane-DDT, milk, niter cake, salt, sugar and sulfur). For each conditioner-material system, they found an optimum amount of conditioner above which flow may not change significantly. Flowability of a material at this level may be markedly different for different conditioners. Peleg and Hollenbach (1984) found considerable change in the bulk density and compressibility of powdered sodium chloride, soy protein and cornstarch when mixed with four conditioners (calcium stearate, sodium silico - aluminate, silicon oxide and tricalcium phosphate) at four concentration levels between 0.1 and 2%. He said that calcium stearate was an effective lubricant, reducing the angle of friction. In contrast, silicon dioxide, a silicate, and tricalcium phosphate had little effect in reducing the angle of internal friction and in some cases even slightly increased it. Chang et al.(1998) measured bulk flow properties (loose bulk density, tapped bulk density, Hausner ratio, angle of repose and shear stress of the powders) of five mixture ratios of potato starch and wheat protein. There were no significant differences in angle of frictions among the tested materials. As the water activity of these materials increased, all bulk flow properties increased except loose bulk density and internal friction angle. Pilpel (1970) investigated the effect of moisture, particle size and flow enhancer on angle of repose for wheat, sand, rape seed, and the effect of moisture content on Jenike flow factor for lactose. The angle of repose increased at higher moisture contents. A small addition (0.5% - 2%) of light magnesia to

starch reduced its angle of repose after it had been exposed to air at 4 to 81% RH for 24 hrs. Flowability, as indicated by the Jenike flow factor, decreased at higher moisture contents for smaller particles. Pilpel (1965) presented the relationship between particle diameter in microns and angle of repose θ to be: $\theta = Ad^{-1} + B$ where A and B are constants whose values for magnesia are 18×10^3 and 32.3 respectively. The angle of repose increased with decreasing particle diameter. The relationship between moisture content and angle of repose is: $\tan \theta = a n^2 + b (M/d_{av}) - c \rho + c'$ where n is the specific surface of the particles relative to a sphere, M is the percentage of moisture in the powder, d_{av} is the average particle diameter, ρ is the specific gravity and a, b, c, and c' are constants. The effects of conditioners on the angle of repose of different powders are complex because of the nature of the conditioner, its concentration, particle size distribution and other variables. Pilpel and Mannheim (1973) investigated the effect of conditioners (calcium stearate and aluminum silicate) on the physical properties (bulk density, compressibility) and flowability of powdered sucrose using the Jenike Flow Factor Tester. The cohesion decreased with the addition of conditioners and at lower moistures. The angle of internal friction decreased with the addition of calcium stearate while aluminum silicate slightly increased the angle.

CHAPTER III

MATERIALS, EQUIPMENT, AND METHODS

Test Materials

Marigold flowers harvested at a private farm in Hydro, Oklahoma were placed in a forced draft oven (Model 350, Isotemp oven, Fisher Scientific Company, USA) at 61°C for 12 hrs to make the detachment of petals easily. The marigold petals were detached from the receptacles by hand. Two kg of marigold petals were ground with 1 mm and 6 mm screens in a Wiley laboratory mill (Model 4, Arthur H. Thomas Corporation, PA) to create two different particle size samples. One kg of each different particle size ground marigold petals was mixed with 3% by weight of tricalcium phosphate, a food grade flow enhancer (D. E. P. Corporation, Rogers, AR), to create samples with 0 % and 3 % flow enhancer. One-half kg samples of ground marigold petals of each combination of particle size and different amount of flow enhancer were placed in a humidity chamber (Model 400-700 CFM Climate-lab, Parameter Generation & Control, Inc., Black Mountain, NC) set at 45% R.H. and 25° C for 48 hrs. Two days later, another set of 0.5 kg samples of each combination of particle size and flow enhancer was placed in the same humidity chamber reset at 75% R. H. and 25° C for 48 hrs, to create samples at a second moisture content.

Physical Properties

Particle size

The particle size of each different-size ground marigold sample was determined on three samples using an ATM sonic sifter Model L3 P series E (ATM Corporation, Milwaukee, WI). Each sample of 25 g ground marigold petals was screened through a set of six different, predetermined sieves at an amplitude level of 6 for 4 minutes. The sieve numbers were 30, 40, 45, 50, 60, 70 for ground marigold petals passing through a 1-mm screen in a Wiley laboratory mill, and 14, 18, 25, 35, 45, 60 for ground marigold petals passing through a 6-mm screen in a Wiley laboratory mill. The average particle size was 0.36 mm for samples passing through the 1-mm screen in the Wiley laboratory mill, and was 0.84 mm for samples passing through the 6-mm screen in the Wiley laboratory mill (See appendix A.2).

Bulk density

Ground marigold petals were poured into a cylindrical container 55 mm inside diameter by 50 mm deep. The volume and the mass of the marigold petals were measured. The bulk density was determined by dividing the mass of the sample by the volume of the sample in the cylindrical container. The samples with 0.37 mm and 0.80 mm average particle size had average bulk densities of 261 and 155 kg/m³, respectively (Hauhouot-O'Hara, et al. 1999).

Moisture content

Lacking a standard method for determining moisture in marigold petals, the standard method for forage or tobacco (ASAE S487, 1998) was used to determine the moisture content of ground marigold petals. Three 15 g samples were dried in a forced draft type oven (Model 350, Isotemp oven, Fisher Scientific Company, USA) at 101°C

for 24 hrs. Moisture content was calculated on a dry basis by dividing the loss in weight during heating by the weight of the dry sample. The moisture content of each sample is shown in Table 3.1.

Table 3.1. Moisture content, dry basis, of ground marigold petals.

Particle Size (mm)	Flow Enhancer (%)	Chamber R. H. (%)	Moisture Content (%)
1	0	45	12.92
1	3	45	12.92
1	0	75	22.29
1	3	75	21.76
6	0	45	11.58
6	3	45	11.16
6	0	75	20.51
6	3	75	20.51

Description of the Shear Testing System

A shear test was conducted to determine the angle of internal friction of the sample using a direct shear cell installed in a universal testing machine (Model No: Renew 1122, Sintech, MTS Systems Corporation, Research Triangle Park, NC). The testing system consists of a direct shear cell, vertical loading block, loading frame, dead weight, a universal testing machine where a normal force is applied and shear test can be done at a constant crosshead speed of 2.000 mm / min (Duffy, 1996), and a computer with TestPad 1.02 software for monitoring and storing the data. The inside diameter of the shear cell is 62.5 mm. The depth of the upper shear cell is 28 mm, and the depth of the lower shear cell is 16 mm. The direct shear cell is shown in Fig.3.1.

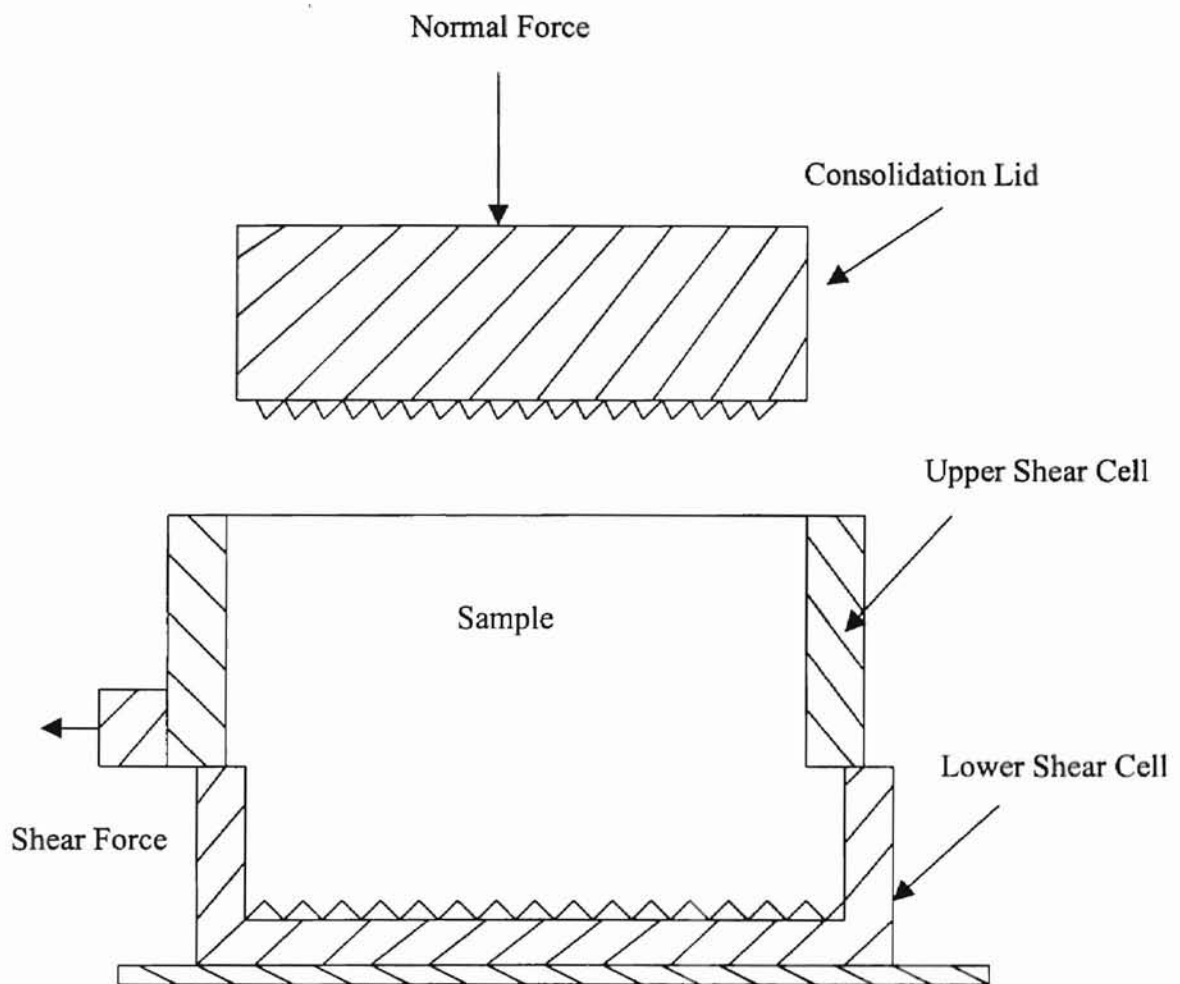


Fig. 3.1. Schematic diagram of the direct shear cell.

Experimental Methods

The upper shear cell was placed on the top of the lower cell. The two alignment pins were inserted through the two holes in the upper shear cell into the lower shear cell and tightened to hold the upper and lower shear cell in place. Initially, 32 g (dry weight) of each sample (the actual weight of each sample is shown in Table 3.2.) was filled into the shear cell using a spoon and was consolidated to attain the desired volume (27 mm in height for 62.5 mm diameter) and desired density (Kocova, 1971) (Pilpel, 1970). The dry weight, the final volume, and the final bulk density were the same for all samples. The number of fillings, the consolidation load and the number of tamping for each sample are shown in Table 3.3.

Table 3.2. Actual weight of ground marigold petals

Treatment	Particle Size (mm)	Flow Enhancer (%)	Chamber R. H. (%)	Moisture Content (%)	Weight of Sample (g)
140	0.37	0	45	12.92	36.136
143	0.37	3	45	12.92	36.136
170	0.37	0	75	22.29	39.134
173	0.37	3	75	21.76	38.963
640	0.80	0	45	11.58	35.705
643	0.80	3	45	11.16	35.572
670	0.80	0	75	20.51	38.563
673	0.80	3	75	20.51	38.563

Table 3.3. Filling, tapping and consolidation of the sample.

Treatment	# Times of fillings	# tamps per filling	Tamp Height (mm)	Consolidation Mass (kg)	Consolidation Time (min)
140	1	10	112	4.0	20
143	1	10	112	4.0	25
170	1	0	0	3.5	25
173	1	0	0	3.5	25
640	7	100	290	4.65	20
643	7	100	290	4.65	20
670	2	55	238	4.0	15
673	2	55	238	4.0	15

The number of fillings, the number of tamps, the consolidation load and the consolidation time were determined by trial and error during preliminary tests as following: If the sample could not be filled into the shear cell at one time, we divided the sample into appropriate number of parts for filling. This approach is used in the procedure for soil shear testing. The consolidation load was determined also in preliminary testing, which was done to determine how much load was needed for 32 g dry weight ground marigold petals in a glass cylinder to produce a constant bulk density. The consolidation time was held within the range of 15 to 25 min. The number of tamps was determined by trial and error until finally the desired volume was attained under the predetermined consolidation load and time. Note that different combinations of #times of fillings, #tamps per filling, tamp height, consolidation load, and time could achieve the same desired volume. After the desired volume was attained, the three vertical set screws were turned to make a gap of 1.6 mm between the upper shear cell and the lower

shear cell to avoid any friction forces between the rings during shearing. The upper shear cell was firmly tightened with the loading block by rotating the horizontal set screws. The two alignment pins were removed and the three vertical set screws were raised into the upper shear cell. The desired normal force was applied to the sample using the dead weight system. The shear test was then run by the universal testing machine for about 15-20 minutes. Digital force and time reading were taken every 0.64 seconds and a diagram of shear force vs. time (or crosshead position) was plotted using the software TestPad1.02. From the plot, the maximum shear force and the time to reach the maximum shear force were determined. For each treatment in Table 3.1, a shear test was run using one of the three predetermined normal forces of 9.8, 19.6, and 29.4N. Each normal force was replicated three times. Each replicate took approximately one and a half hours.

Calibration of the shear testing system

Commercial refined sugar was used as the standard reference material for calibrating the system. This calibration test was done at the beginning of each week. Eighty grams of refined sugar was poured into the shear cell. The tamping cylinder was raised to 290 mm and the sample was tamped 20 times. A normal force of 19.6N was applied to the sample. The maximum shear force was recorded and compared with the results from previous weeks. If there was any deviation greater than 5%, then the load cell was recalibrated. This however was never necessary during the eight weeks of testing.

Data Analysis

The data were analyzed using statistical software (SAS and SYSTAT). Analysis of variance (ANOVA) was used to investigate whether there were significant different mean values of the angle of the internal friction and cohesion among treatments. Fischer's Least Significant Difference (LSD) was used to do multiple comparison. Two – way interactions and the three – way interaction also were investigated.

CHAPTER IV

RESULTS AND DISCUSSION

During a shear test, the shear force versus time curve was recorded by the computer, as shown by a typical graph in Fig. 4.1. The data were converted to a graph of shear stress versus displacement by multiplying by constants. Force was converted to shear stress: $\tau = F/A$, where τ = shear stress (kPa), F = shear force (N), A = initial cross-sectional area of the specimen (mm^2) (ASTM, 1998). Time was converted to displacement by multiplying by the testing machine's crosshead speed.

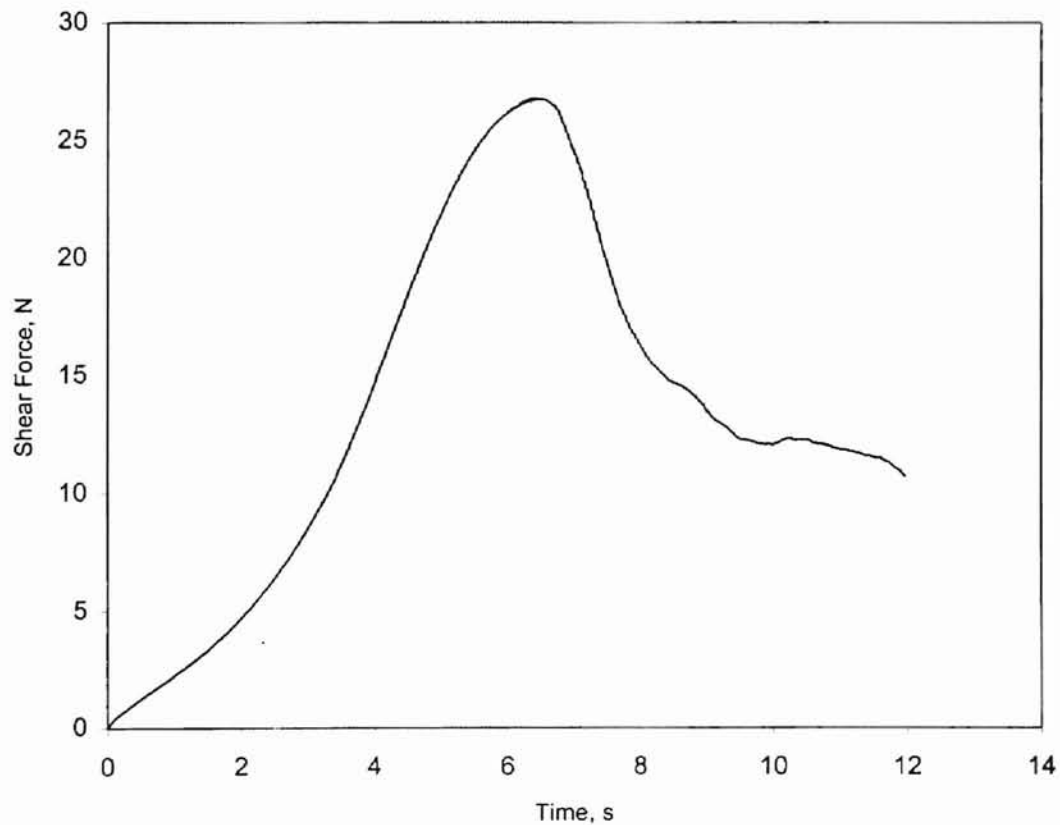


Fig.4.1. A typical shear force vs. time graph.

In the curve, the shear stress first increases with displacement until it reaches a maximum stress and then the shear stress decreases. According to ASTM Standards D3080 (1998), the stress condition at failure is often taken to correspond to the maximum shear stress attained, or the shear stress at 15 to 20 percent of horizontal displacement of the top and bottom shear box halves. For this study the maximum shear stress was selected as the failure stress.

The yield locus can be used to compare the flowability of different sample treatments. To get a yield locus, the maximum shear stresses under three normal stresses less than the consolidating stress were measured (Table 4.1). A yield locus is a plot of the maximum (or failure) shear stress versus the normal stress acting on the shear plane during the test. It gives the stress conditions needed to produce flow for the powder when compacted to a fixed bulk density. A typical yield locus is shown in Fig. 4.2. The slope of the linear regression line represents the angle of internal friction (Φ) (Negi, 1987), which is the interparticle friction angle as a bulk solid starts to slide on itself at the onset of flow. The intercept (C) of the regression line represents the cohesion of the test material. The angles of internal friction and cohesion of sample for each treatment and each replication are shown in Table 4.2. The mean values and standard deviations of Φ and C are shown in Table 4.3.

Table 4.1 – Normal stresses and corresponding maximum shear stresses for each treatment

treatment*	normal (kPa)	shear (kPa)	treatment	normal (kPa)	shear (kPa)
1401	3.194	4.612	6401	3.194	6.288
	6.389	7.409		6.389	9.433
	9.583	9.524		9.583	12.402
1402	3.194	4.778	6402	3.194	6.030
	6.389	7.106		6.389	9.430
	9.583	10.323		9.583	12.546
1403	3.194	5.072	6403	3.194	6.030
	6.389	7.481		6.389	9.430
	9.583	10.313		9.583	12.546
1431	3.194	16.550	6431	3.194	7.986
	6.389	25.990		6.389	12.533
	9.583	35.240		9.583	16.131
1432	3.194	17.120	6432	3.194	8.755
	6.389	26.900		6.389	12.210
	9.583	37.380		9.583	16.868
1433	3.194	18.190	6433	3.194	7.510
	6.389	25.960		6.389	11.411
	9.583	35.860		9.583	15.114
1701	3.194	4.609	6701	3.194	3.540
	6.389	7.256		6.389	6.369
	9.583	9.889		9.583	8.442
1702	3.194	4.355	6702	3.194	2.870
	6.389	7.777		6.389	5.991
	9.583	10.740		9.583	8.038
1703	3.194	4.811	6703	3.194	3.087
	6.389	7.536		6.389	5.502
	9.583	10.492		9.583	7.790
1731	3.194	4.804	6731	3.194	13.33
	6.389	7.640		6.389	22.55
	9.583	11.193		9.583	29.27
1732	3.194	4.628	6732	3.194	13.25
	6.389	7.657		6.389	21.39
	9.583	11.421		9.583	29.23
1733	3.194	4.893	6733	3.194	11.87
	6.389	8.080		6.389	18.18
	9.583	10.958		9.583	27.36

*Treatment ID code: First digit is particle size. Second digit is MC. Third digit is % flow enhancer. Fourth digit is replicate number.

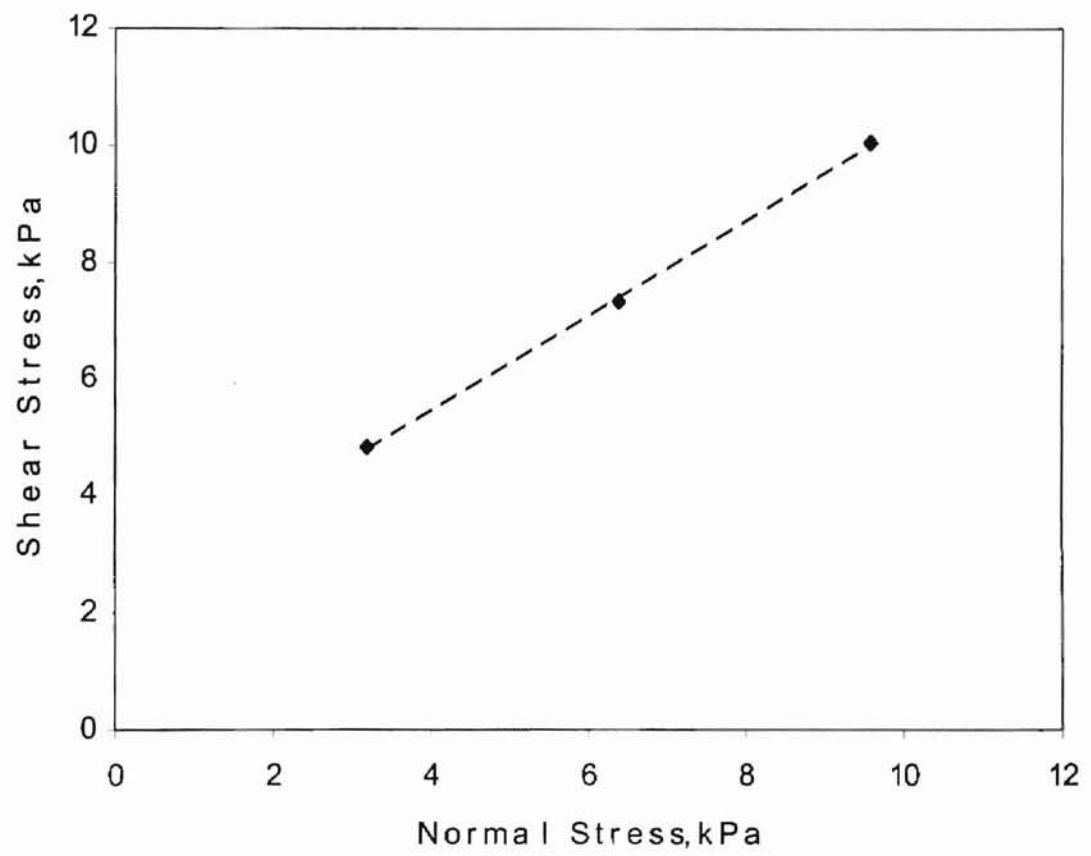


Fig 4.2 A typical yield locus for shear stress vs. normal stress.

Table 4.2 – Angles of internal friction and cohesion coefficients for each treatment.

Treatment	Angle of internal friction, Φ (°)	Cohesion (kPa)
1401	37.56	2.270
1402	40.96	1.858
1403	39.37	2.381
1431	43.64	2.359
1432	45.95	2.240
1433	42.04	2.934
1701	44.99	1.239
1702	39.57	1.971
1703	41.65	1.932
1731	45.00	1.491
1732	46.76	1.109
1733	43.52	1.911
6401	43.74	3.260
6402	45.56	2.820
6403	43.27	3.230
6431	51.89	4.071
6432	51.78	4.498
6433	49.97	3.741
6701	37.50	1.215
6702	38.97	0.465
6703	36.36	0.757
6731	39.12	1.883
6732	39.19	1.731
6733	38.32	1.189

Table 4.3 – Means and standard deviations of angle of internal friction and cohesion coefficients.

Treatment *	Angle of internal friction, Φ (°)	Cohesion, C (kPa)
140	39.29 ± 1.70	2.169 ± 0.276
143	43.87 ± 1.97	2.511 ± 0.371
170	42.07 ± 1.21	1.714 ± 0.412
173	45.09 ± 1.08	1.504 ± 0.401
640	44.19 ± 2.73	3.103 ± 0.246
643	51.21 ± 1.62	4.103 ± 0.380
670	37.61 ± 1.31	0.812 ± 0.378
673	38.87 ± 0.48	1.601 ± 0.365

* Treatment ID code: First digit is particle size. Second digit is moisture content.

Third digit is % flow enhancer.

Effect of particle size

The effects of particle size on the angle of internal friction and cohesion of marigold petals are shown in Fig. 4.3 and Fig. 4.4, respectively. The angle of internal friction and cohesion increased with larger particle size when relative humidity is 45% with or without flow enhancer. The angle of internal friction increased by 12.47% with particle size at 0% TCP, 45%RH, and increased by 16.73% with particle size at 3% TCP, 45%RH. The cohesion increased by 43.04% with particle size at 0% TCP, 45%RH, and increased by 63.42% with particle size at 3% TCP, 45%RH.

The angle of internal friction decreased with larger particle size when relative humidity is 75% with or without flow enhancer. The angle of internal friction decreased by 10.60% with particle size at 0% TCP, 75%RH and decreased by 13.78% with particle

size at 3% TCP, 75%RH. Cohesion decreased by 52.61% with larger particle at 0% TCP, 75%RH, but increased by 6.46% with larger particle size at 3% TCP, 75%RH.

The varying effect of particle size on angle of internal friction may be due to a significant interaction between particle size and moisture content. With more moisture, the film on the surface of a particle has a greater tendency to act as a lubricant. Small particle size also provides more surface area available for any surface-related factors.

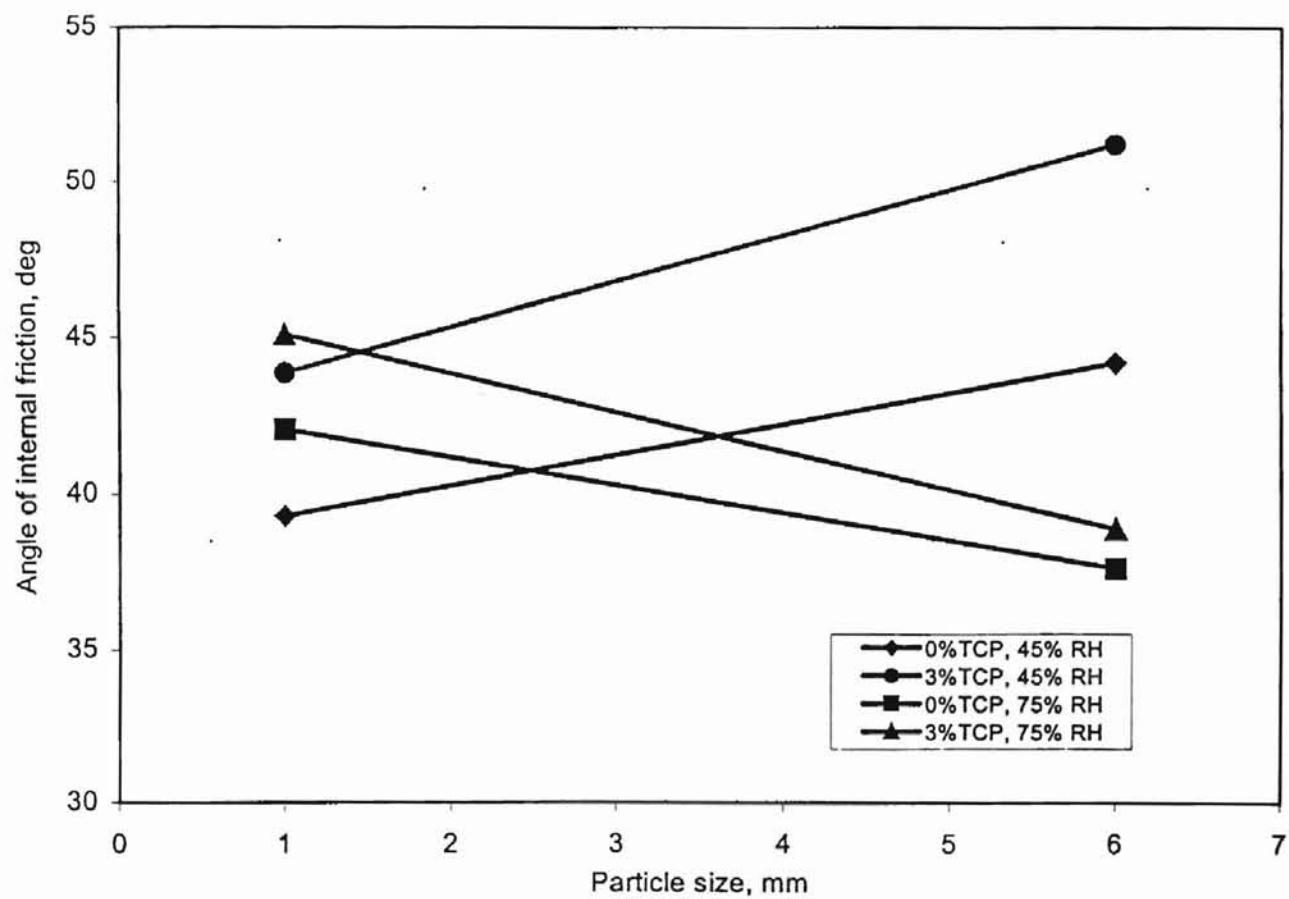


Fig. 4.3 The effect of particle size on the angle of internal friction.

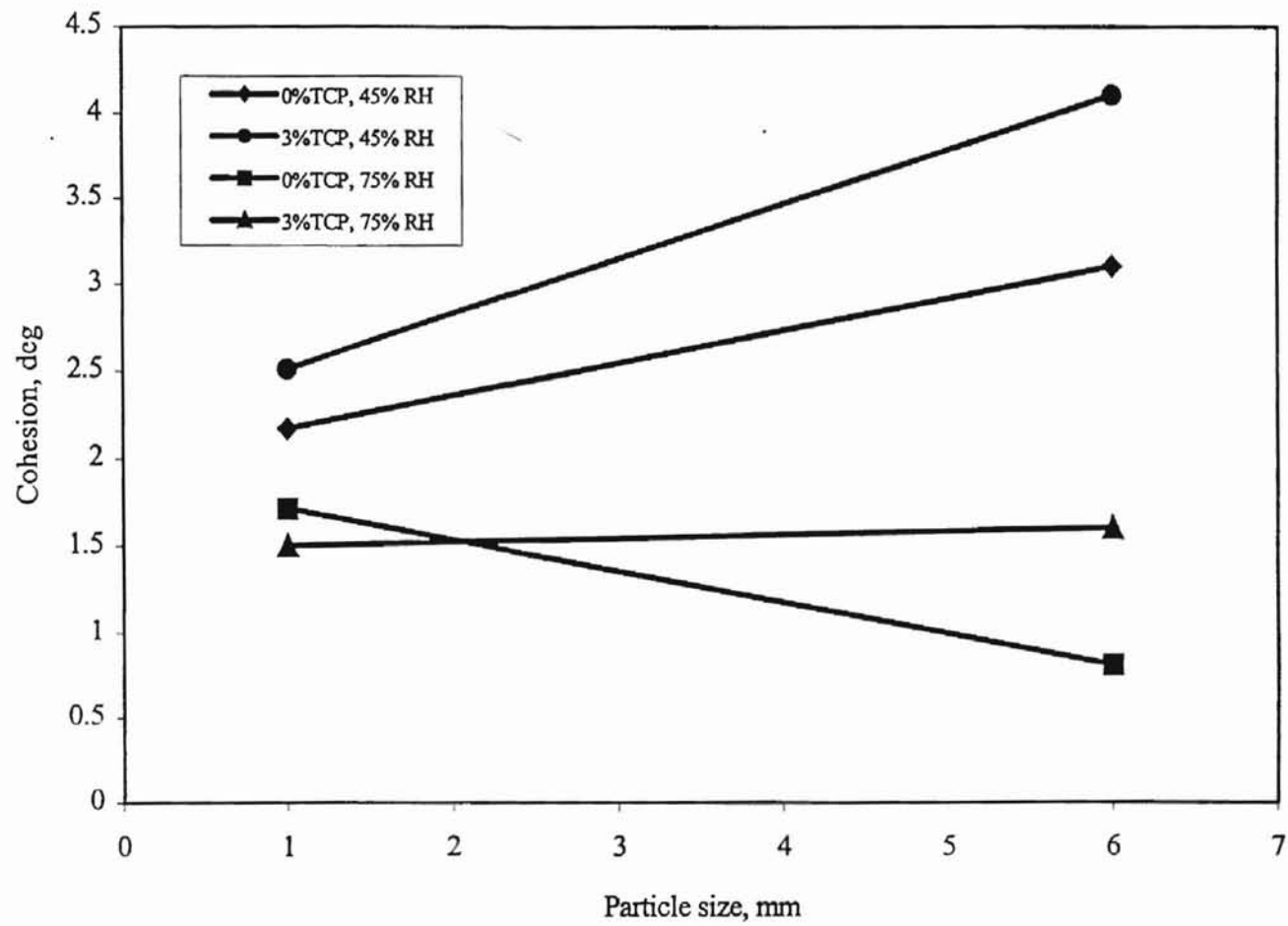


Fig. 4.4 The effect of particle size on cohesion.

Effect of moisture content

The effects of moisture content on the angle of internal friction and cohesion of test materials are shown in Fig. 4.5 and Fig. 4.6, respectively. The angle of internal friction increased with higher moisture content for small particles (1-mm) with or without flow enhancer. The angle of internal friction increased by 7.07% at 0% TCP and by 2.77% at 3% TCP for 1-mm particles. The angle of internal friction decreased with higher moisture content for large particles (6-mm) with or without flow enhancer. The angle of internal friction decreased by 14.89% at 0% TCP and by 24.09% at 3% TCP for 6-mm particles. Peleg (1973) explained that the liquid layer formed on the powder surface due to moisture uptake acted as a lubricant when shear force was applied and thus decreased the angle of internal friction for powdered sucrose.

Cohesion decreased with higher moisture content. Cohesion decreased by 21.00% at 0% TCP and by 40.11% at 3% TCP for 1-mm particles. Cohesion decreased by 73.83% at 0% TCP and by 60.98% at 3% TCP for 6-mm particles.

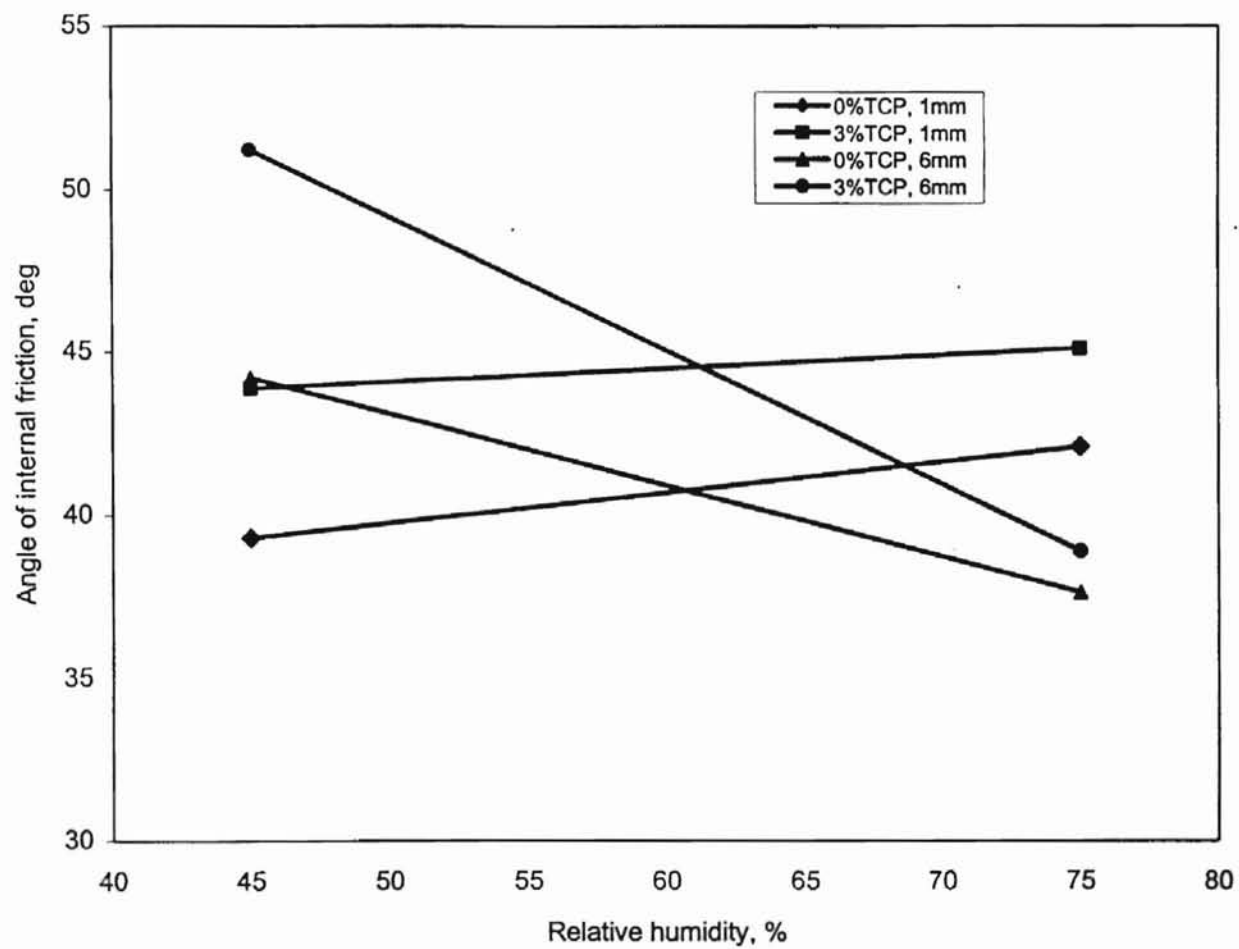


Fig. 4.5 The effect of moisture content (RH in conditioning chamber) on the angle of internal friction.

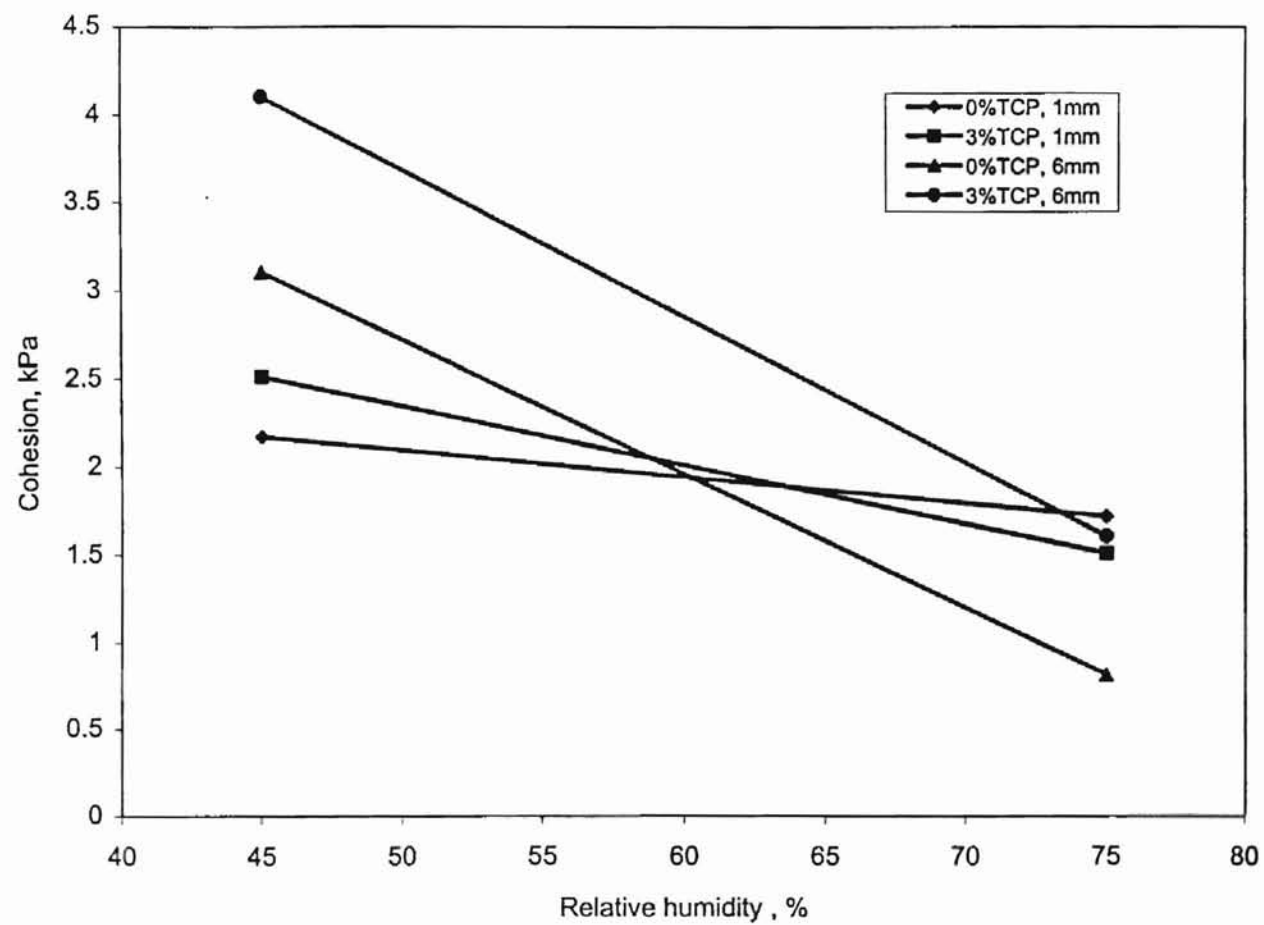


Fig. 4.6 The effect of moisture content (RH in conditioning chamber) on cohesion.

Effect of flow enhancer

The effects of flow enhancer on the angle of internal friction and cohesion of marigold petals are shown in Fig. 4.7 and Fig. 4.8, respectively. The angle of internal friction increased with addition of flow enhancer. Cohesion also increased with addition of flow enhancer except for smaller particles at higher moisture content (treatment 170 and treatment 173). This may be caused by different surface properties of ground marigold petals after adding tricalcium phosphate as noted by Peleg and Hollenbach (1984).

The angle of internal friction increased by 11.66% and the cohesion increased by 15.74% with addition of 3% flow enhancer at 45%RH, 1-mm particles. The angle of internal friction increased by 7.18% while cohesion decreased by 12.26% with addition of 3% flow enhancer at 75%RH, 1-mm particles. The angle of internal friction increased by 15.89% and the cohesion increased by 32.23% with addition of 3% flow enhancer at 45%RH, 6-mm particles. The angle of internal friction increased by 3.37% and cohesion increased by 97.12% with addition of 3% flow enhancer at 75%RH, 6-mm particles.

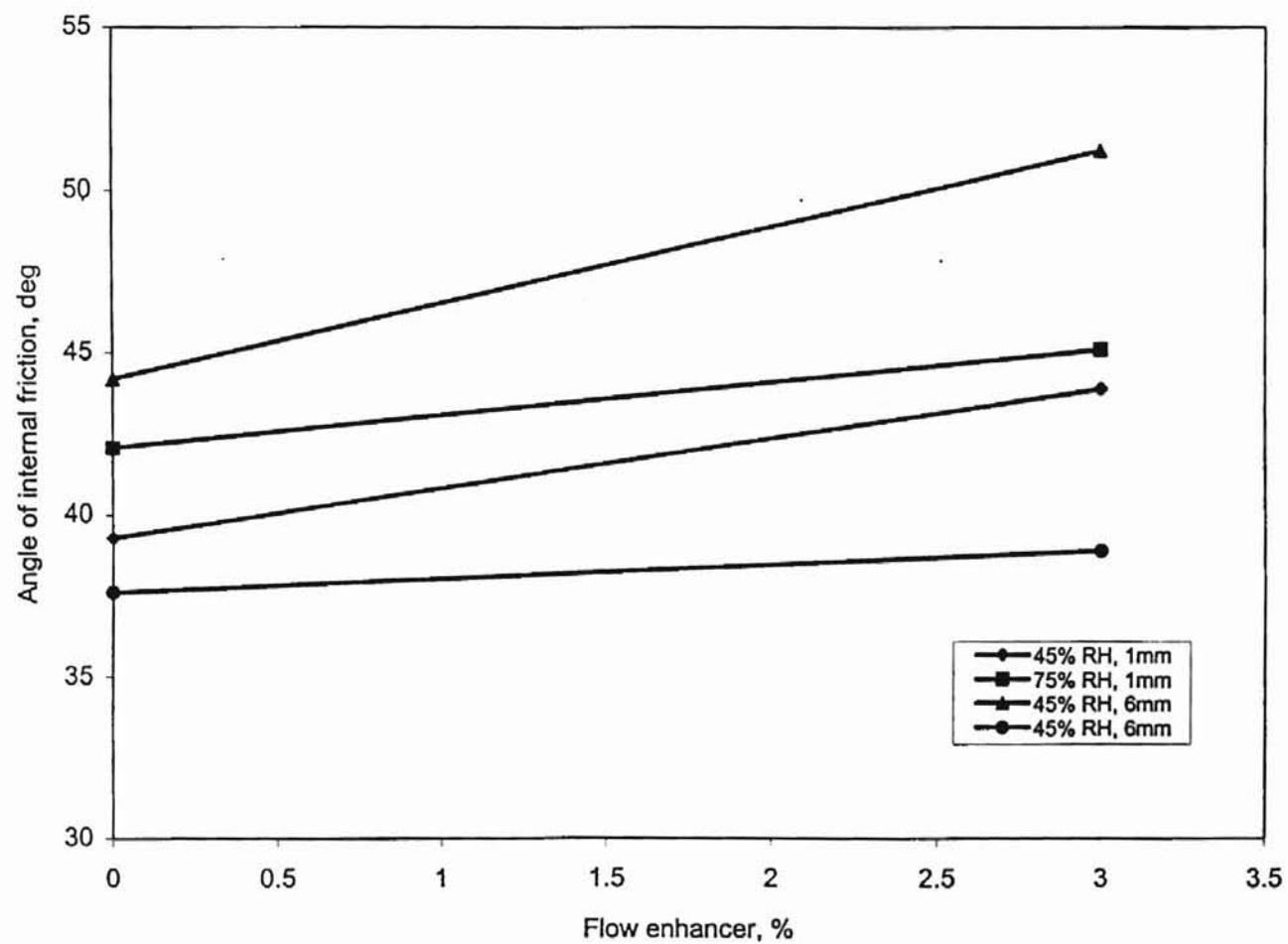


Fig. 4.7 The effect of flow enhancer on the angle of internal friction.

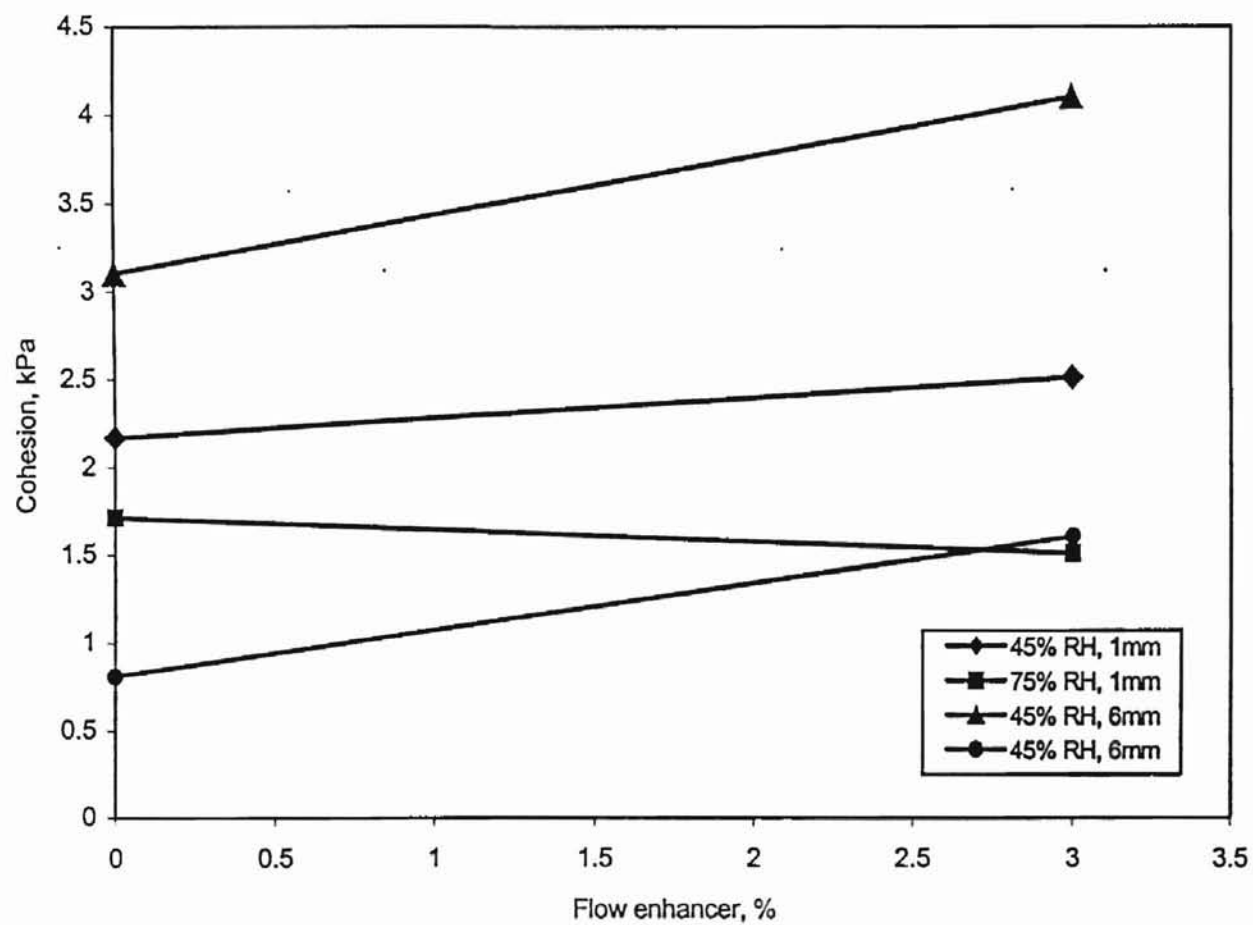


Fig. 4.8 The effect of flow enhancer on the cohesion.

Main effects

The plot of main effects on angle of internal friction indicated that changes in particle size had least effect while changes in moisture content and flow enhancer had more effect (Fig. 4.9). ANOVA (Table 4.4) shows that particle size had no significant effect on the angle of internal friction ($P = 0.569$). Moisture content ($P = 0.0001$) and flow enhancer ($P = 0.0001$) both had significant effects on the angle of internal friction. The plot of main effects on cohesion indicated that changes in moisture content had the most effect on cohesion while changes in particle size and flow enhancer had less effect. (Fig. 4.10). ANOVA (Table 4.5) shows that particle size, moisture content, and flow enhancer all had significant effect on cohesion of ground marigold petals. Moisture content had the most effect ($P = 0.0001$) while particle size ($P = 0.009$) and flow enhancer ($P = 0.005$) had less effect on cohesion.

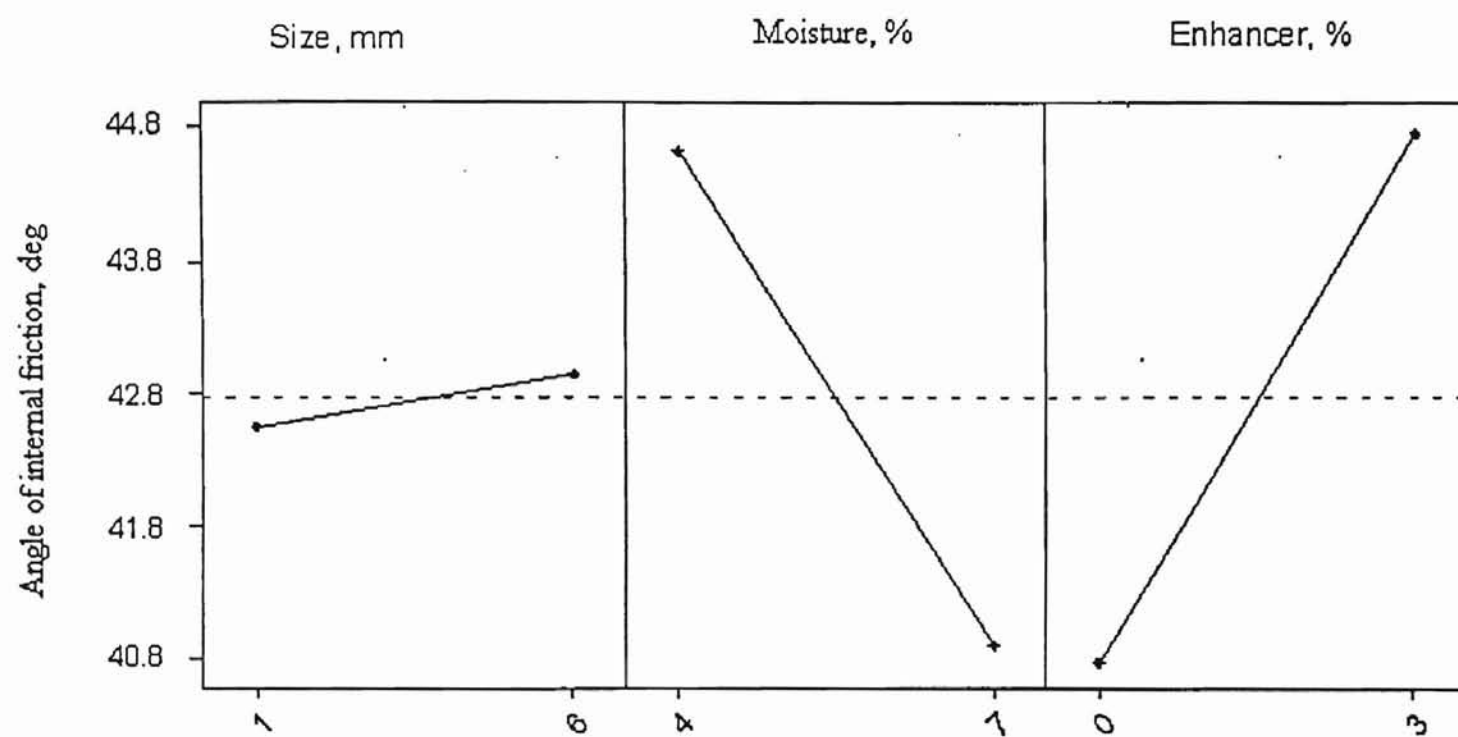


Fig.4.9 Main effect plot for angle of internal friction.

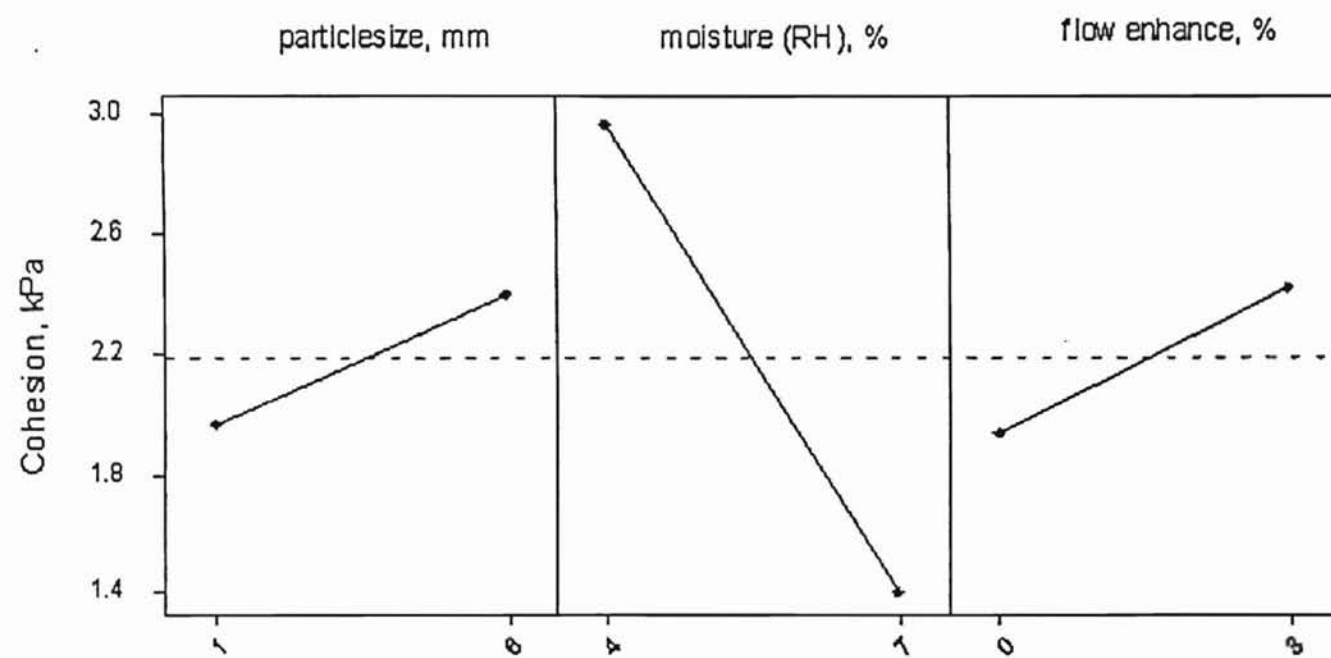


Fig.4.10 Main effect plot for cohesion.

Effect of interactions

Before drawing conclusions regarding the main effects, we should consider interactions between parameters. Analysis of variance (ANOVA) for angle of internal friction and cohesion (Table 4.4 and Table 4.5) showed no significant three – way interaction. For angle of internal friction, there were significant two – way interactions between particle size and moisture content, between moisture content and flow enhancer but not between particle size and flow enhancer. For cohesion, there were significant two – way interactions between particle size and moisture content, between particle size and flow enhancer but not between moisture content and flow enhancer.

Table 4.4- Analysis of variance for angle of internal friction.

Source	Sum-of-Squares	df	Mean-Square	F-ratio	P
SIZE	0.905	1	0.905	0.338	0.5661
MOISTURE	83.552	1	83.552	31.181	0.0001
ENHANCER	94.724	1	94.724	35.351	0.0001
SIZE*MOISTURE	196.768	1	196.768	73.433	0.0001
SIZE*ENHANCER	0.177	1	0.177	0.066	0.8019
MOISTURE*ENHANCER	20.057	1	20.057	7.485	0.0147
SIZE*MOISTURE*ENHANCER	6.615	1	6.615	2.469	0.1361

Table 4.5- Analysis of variance for cohesion.

Source	Sum-of-Squares	df	Mean-Square	F-ratio	P
SIZE	1.112	1	1.112	8.678	0.0095
MOISTURE	14.678	1	14.678	114.597	0.0001
ENHANCER	1.382	1	1.382	10.789	0.0047
SIZE*MOISTURE	4.159	1	4.159	32.472	0.0001
SIZE*ENHANCER	1.030	1	1.030	8.045	0.0119
MOISTURE*ENHANCER	0.218	1	0.218	1.704	0.2101
SIZE*MOISTURE*ENHANCER	0.043	1	0.043	0.339	0.5689

Two way interaction plots for angle of internal friction and cohesion are shown in Fig. 4.11 and 4.12, respectively. When lines in the figure cross, this indicates there is interaction. The amount of crossing indicates the degree of interaction. Parallel or nearly parallel lines indicate lack of interaction. The interaction plots graphically show what is given numerically by ANOVA. For angle of internal friction (Fig.11), there is no interaction between particle size and flow enhancer. There is little interaction between moisture content and flow enhancer, but there is large interaction between particle size and moisture content. For cohesion (Fig.12), there is no interaction between moisture content and flow enhancer. Particle size and moisture content interact more than particle size and flow enhancer. The conclusion from this study is that particle size by moisture content is the most important interaction and may be as important as the main effects.

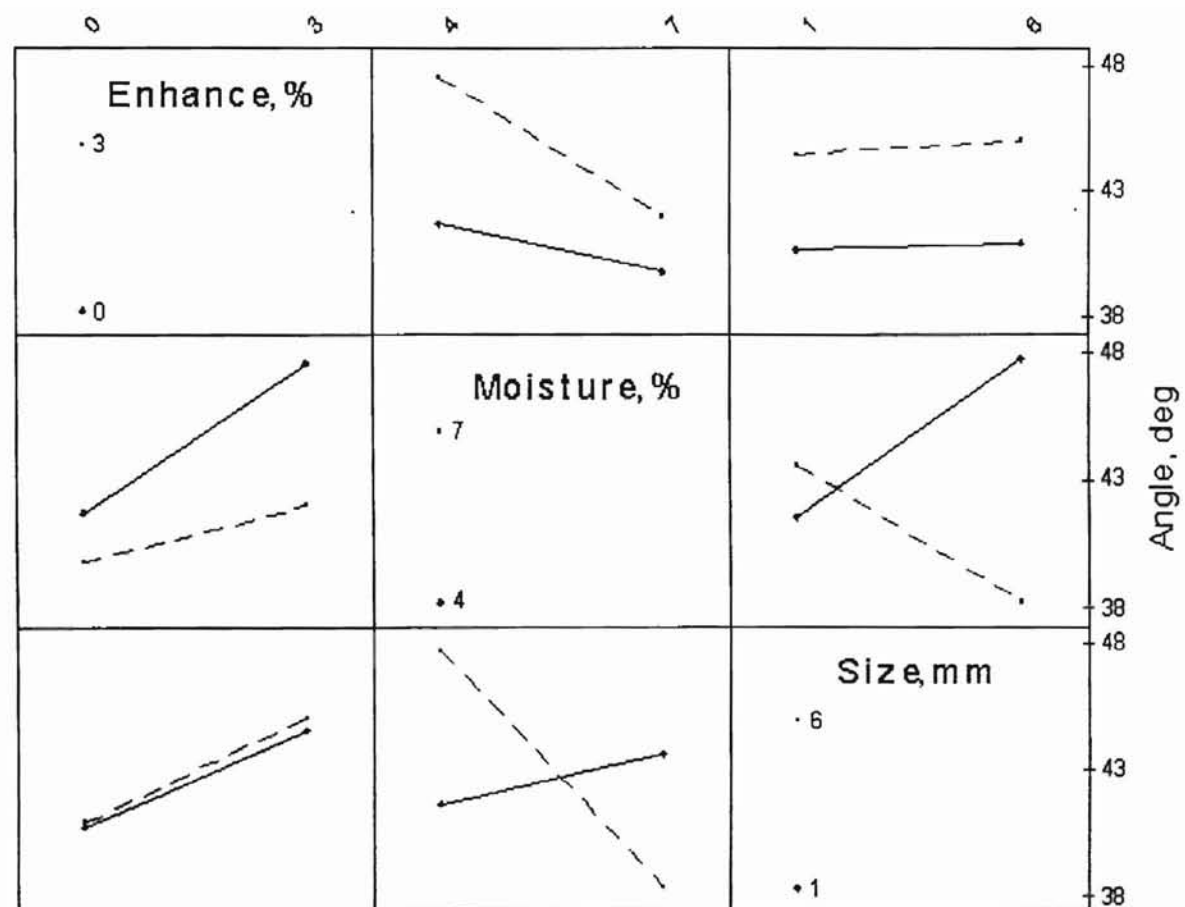


Fig. 4.11 Interaction plot for angle of internal friction.

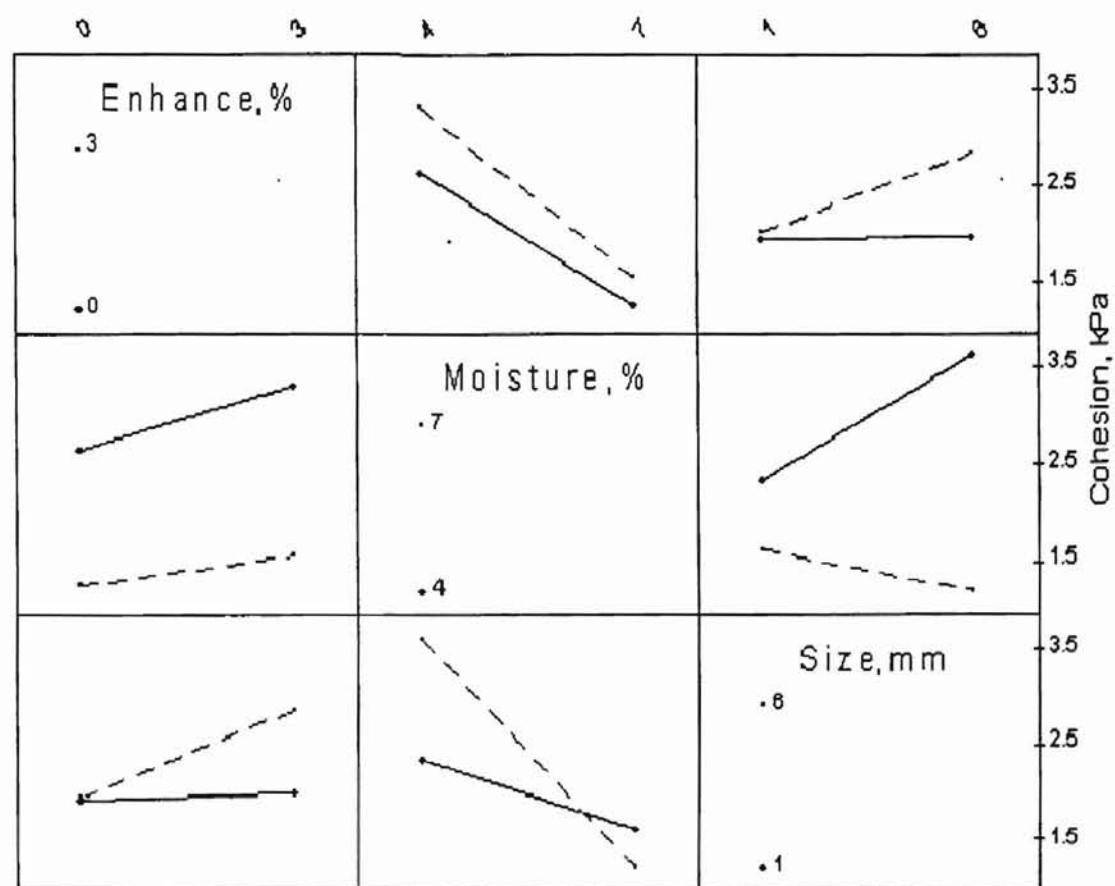


Fig. 4.12 Interaction plot for cohesion.

Regression Analysis

The regression equations with only main effects are as follows.

The regression equation for angle of internal friction (°) is:

$$\text{Angle} = 47.983 + 0.078 \text{ particle size} - 0.124 \text{ moisture} + 1.324 \text{ flow enhancer} \quad (4.1)$$

Where particle size has units of mm, moisture content corresponding to equilibrium RH in units of %RH, and flow enhancer has units of % by weight.

The r^2 for this equation is 0.402.

The regression equation for cohesion (kPa) is:

$$\text{Cohesion} = 4.777 + 0.086 \text{ particle size} - 0.052 \text{ moisture} + 0.160 \text{ flow enhancer} \quad (4.2)$$

The r^2 for this equation is 0.696.

The regression equations with the main effect and two – way interactions are as follows.

The regression equation for angle of internal friction (°) is:

$$\begin{aligned} \text{Angle} = & 28.412 + 4.625 \text{ particle size} + 0.204 \text{ moisture} + 3.628 \text{ flow enhancer} - 0.076 \\ & \text{moisture*particle size} + 0.023 \text{ enhancer*particle size} - 0.041 \text{ enhancer*moisture.} \end{aligned} \quad (4.3)$$

The r^2 for this equation is 0.889.

The regression equation for cohesion (kPa) is:

$$\begin{aligned} \text{Cohesion} = & 2.354 + 0.669 \text{ particle size} - 0.007 \text{ moisture} + 0.221 \text{ flow enhancer} - 0.011 \\ & \text{moisture*particle size} + 0.055 \text{ enhancer*particle size} - 0.004 \text{ enhancer*moisture.} \end{aligned} \quad (4.4)$$

The r^2 for this equation is 0.915.

For the angle of internal friction regression equations, including the two-way interaction terms improves the r^2 from 0.402 to 0.889 and for cohesion, the improvement is from 0.696 to 0.915.

Test at different mass

An additional test was conducted to compare the results obtained by the method used to fill the shear cell with another method. This test was done starting with the same initial volume and the same tamping condition as that of treatment 143 but a different mass and different final volume. To attain this condition required 22.5g of sample. The angle of internal friction and cohesion for this sample are given in table 4.6:

Table 4.6 Angle of internal friction and cohesion of treatment 143 by alternative shear filling method

Rep. #	normal(kPa)	shear(kPa)	angle of internal friction, deg	cohesion(kPa)
1	3.19	6.34	44.25	3.36
	6.39	9.85		
	9.58	12.56		
2	3.19	6.13	43.94	3.13
	6.39	9.42		
	9.58	12.29		
3	3.19	6.01	41.84	3.24
	6.39	9.12		
	9.58	11.73		
			43.34 \pm 1.31	3.24 \pm 0.12

For treatment 143 with 32g of material, the angle of internal friction was $43.87 \pm 1.97^\circ$ and cohesion was 2.511 ± 0.371 kPa. Thus, with less mass, the angle of internal friction decreased by 1.21% and the cohesion increased by 29.1%. The differences on angle of internal friction between these two methods were less than the amounts needed to be statistically significant.

Further Discussion

After the shearing test, the sample was either caked or had loose particles for different treatments. For small particles with low moisture content, there was no caking of the sample. For small particles with high moisture content, the sample caked a little bit. For large particles with low and high moisture content, the sample was caked well after testing.

An attempt was made to estimate the height of a column of ground marigold petals that would produce the same bulk density as that obtained during the consolidated shear tests. From the literature, Jofriet and Daynard (1982) determined the average dry – matter density of 15.5% M.C. cracked shelled corn was 606 kg / m^3 and 528 kg / m^3 for 30% M.C. for all sizes of silo. The average bulk density of 30% M.C. ground shelled corn in a 3.7 m diameter by 9.1 m high silo was about 890 kg / m^3 . They developed an equation for the density at a depth below the top of the silage in a silo, which is written as:

$$\gamma(z) = \gamma_0 + p (1 - e^{-qz}) \quad (4.5)$$

Where $\gamma(z)$ is the density at a depth z below the top of the silage (kg/ m^3), γ_0 is loose bulk density (kg/m^3), z is depth below the top of the silage (m), and p and q are material parameters. A typical graph of this equation is shown in Fig.4.13.

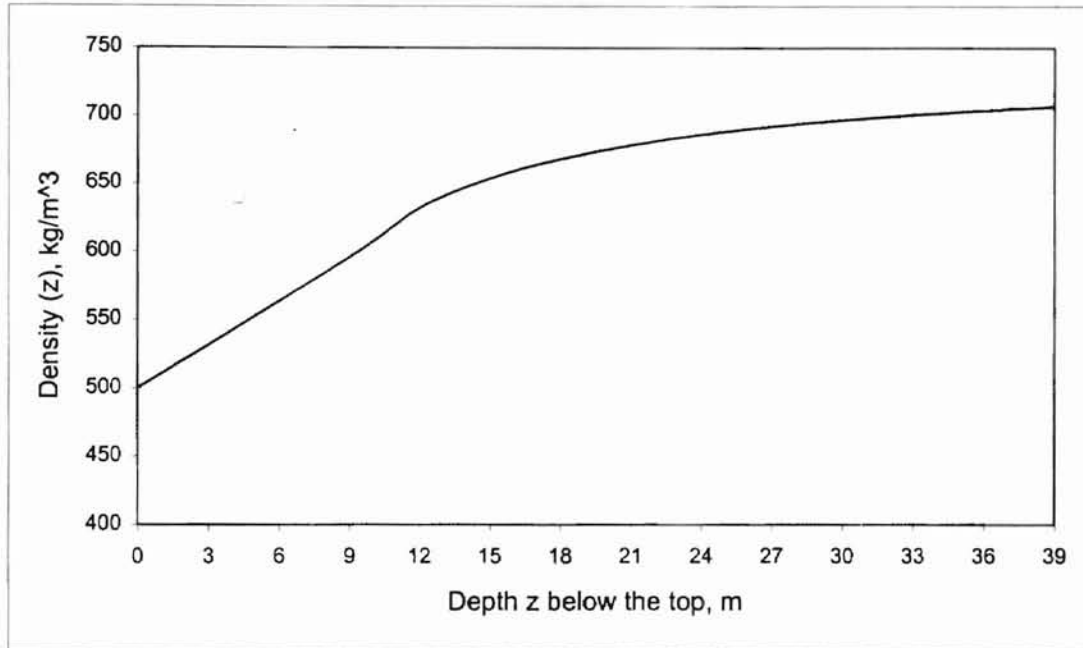


Fig. 4.13 The graph of relationship between depth and density in silage.

For ground ear corn, $\gamma_0 = 400 \text{ kg/m}^3$, $p = 240 \text{ kg/m}^3$, $q = 0.16 \text{ m}^{-1}$. Similar p and q were obtained for ground shelled corn though γ_0 was quite different. We assumed the same coefficients, p and q for ground marigold petals. The loose bulk density for 1-mm particles of ground marigold petals was 261 kg/m^3 (Hauhouot-O'Hara, 1999). In the current experiment, the compacted bulk density was 436 kg/m^3 for small particles with lower moisture content, and 472 kg/m^3 for small particles with higher moisture content. Using these data in equation (4.5), the depth z was computed. Densities used in the shear cell tests corresponded to density of ground marigold petals as predicted by equation (4.5) for a 8.18 m high bin for small particles with lower moisture content, and 13.08 m high bin for small particles with higher moisture content. Because of the low bulk density of 6-mm particles and the flattening out of the curve at depths greater than 30 m, compaction in the shear cell corresponded to the density predicted by equation (4.5) for a very high (infinite) bin.

CHAPTER V

SUMMARY AND CONCLUSIONS

Summary

Of the three parameters, particle size had the least effect while flow enhancer had the most effect on the angle of internal friction. Moisture content had the most effect on cohesion while particle size had the least effect. This indicates that the two particle sizes tested had a similar effect on flowability of ground marigold petals. Higher moisture content decreased the cohesion of ground marigold petals. The similar result was obtained by Pilpel (1970). Pilpel reported work by Harwood saying that for samples that had been highly consolidated, the moist samples had a lower tensile strength than the dry ones, although, the tensile strength and cohesiveness of relatively loose packed lactose and rose increased with moisture content. Moisture affected (either increased or decreased) cohesion depending on the concentration of samples and the extent to what the sample had been packed or consolidated. Duffy (1999) found that there was no observable trend for the angle of internal friction as a function of moisture content for coated cottonseeds, shelled corn and soybeans at moisture contents between 8.3% and 12.8%. Particles of large size and higher moisture content with no flow enhancer had the lowest angle of internal friction. Adding flow enhancer increased the angle of internal friction by 1.1° - 7.0° and increased the cohesion by 0.342 kPa - 1.000 kPa, except for small particles at high moisture contents. These results may be caused by the interaction among parameters and the physical properties of the flow enhancer.

Particle size and moisture content had an interacting effect on the angle of internal friction and cohesion. Large particles at low moisture contents had higher angle of internal friction and cohesion and likewise at higher moisture contents had lower angle of internal friction and cohesion.

Conclusions

1. Particle size had the least effect while low flow enhancer had the most effect on the angle of internal friction.
2. Moisture content had the most effect while particle size had the least effect on cohesion.
3. Particle size and moisture content had an interacting effect on the angle of internal friction and cohesion. Large particles at low moisture contents had higher angle of internal friction and cohesion and likewise at higher moisture contents had lower angle of internal friction and cohesion.
4. Larger particles and lower moisture content with 3% flow enhancer had the highest angle of internal friction (51.2°).
5. The regression equation for angle of internal friction had $r^2 = 0.89$ when the interaction terms were included compared to $r^2 = 0.40$ with only the main effects. The r^2 for the cohesion regression equation was improved from 0.70 to 0.92 by adding the interaction terms.

CHAPTER VI

RECOMMENDATIONS FOR FUTURE STUDY

The following are suggested for further study:

1. Use more levels or wider range of the parameters; particle size, moisture content, and flow enhancer.
2. Consider other parameters such as temperature and consolidation time.
3. Consider the effects of particle size distribution on the flowability of ground marigold petals.
4. Use another type of flow enhancer besides tricalcium phosphate (TCP).
5. Use a different procedure for the direct shear experiment; i.e., use constant consolidation stress in placing samples in the shear cell instead of using constant final bulk density.

BIBLIOGRAPHY

ASAE Standards, 1999. S358.2, Moisture Measurement – Forages. St Joseph, Mich.: ASAE.

Annual Book of ASTM Standards (V04.08), 1998. D3080-90, Standard test method for direct shear test of soils under consolidated drained conditions. West Conshohocken, PA.: ASTM.

Chang, K.S., D.W.Kim, S.S.Kim and M.Y.Jung. 1998. Bulk flow properties of model food powder at different water activity. *International Journal of Food Properties*, 1(1): 45-55.

Delgado, F.V. and O.Paredes. 1998. Effects of sunlight illumination of marigold flower meals on egg yolk pigmentation. *Journal of Agricultural Food Chemistry*, 46(2): 698-706.

Duffy, S.P. and V.M.Puri. 1996. Flow parameters and flow functions for confectionery sugar and detergent powder at two moisture contents. *Applied Engineering in Agriculture*, 12(5): 601-606.

Duffy, S.P. and V.M.Puri. 1999. Measurement and comparison of flowability of coated cottonseeds, shelled corn and soybeans at three moisture contents. *Transactions of the ASAE*, 42(5): 1423-1427.

Gentry, E.G., B.J.Deere and S.A.Yount. 1970. Status of the flowability test for core sand mixtures. *AFS Transactions*, 78: 33-36.

Haaker, G.and W.J.A.Wiersma-van Schendel. 1993. A constant volume shear tester. *Bulk Solids Handling: the International Journal of Storing and Handling Bulk Materials*, 13(1): 129-133.

Hauhouot-O'Hara, M., G.H.Brusewitz, and Y.Zou. 1999. Flowability of uncompacted ground marigold petals as a function of particle size, moisture content, and flow enhancer. *Applied Engineering in Agriculture*, 15(4): 319-322.

Hollenbach, A.M. and M.Peleg. 1983. Interparticle surface affinity and the bulk properties of conditioned powders. *Powder Technology*, 35(1): 51-62.

Irani, R.R., C.F.Callis and T.Liu. 1959. Flow conditioning and anticaking agents. *Industrial and Engineering Chemistry*, 51(10): 1285-1288.

Jenike, A.W. 1964. Bulletin No.123-Storage and flow of solids, pp 10-56. Utah Engineering Station. University of Utah.

- Jenike, A.W. and J.W.Carson. 1987. Measurement principles of the flowability of powders. *Advances in Ceramics*, 21: 759-766.
- Kamath, S., V.M.Puri, H.B.Manbeck and R.Hogg. 1993. Flow properties of powders using four testers-measurement, comparison and assessment. *Powder Technology* 76 (3): 277-289.
- Kamath, S., V.M.Puri and H.B.Manbeck. 1994. Flow property measurement using the Jenike cell for wheat flour at various moisture contents and consolidation times. *Powder Technology*, 81 (3): 293-297.
- Kandala, R.N. and V.M.Puri. 1998. Comparison of flowability measurements of powders at low pressures using two testers. Presented at the July 12-16, 1998 ASAE meeting. Paper No. 984020. ASAE, 2950 Niles Rd., St Joseph, MI 49085-9659 USA.
- Kocova, S. and N.Pilpel. 1972. The failure properties of lactose and calcium carbonate powders. *Powder Technology*, 5(6): 329-343.
- Kozler, J.and J.Novosad. 1989. A method for testing the flowability of fertilizers. *Bulk Solids Handling*, 9(1): 43-48.
- Kurz, H.P. and G.Munz. 1975. The influence of particle size distribution on the flow properties of limestone powders. *Powder Technology*, 11(1): 37-40.

Lai, C.C., G.Seymour, G.Gilbert and C.H.Mannheim. 1985. Effect of composition on the flow properties of egg powders. *Journal of Food Science*, 50(6): 1618-1620.

Lai, C.C., S.G.Gilbert and C.H.Mannheim. 1986. Effect of flow conditioners on water sorption and flow properties of egg powder. *Journal of Food Engineering*, 5(4): 321-333.

Ludlow, D.K. and N.R.Aukland. 1990. Caking and flowability problems of sugar in a cold environment. *Powder Handling and Processing*, 2(1): 21-24.

Murthy, C.T. and S. Bhattacharya. 1998. Moisture dependant physical and uniaxial compression properties of black pepper. *Journal of Food Engineering*, 37(2): 193-205.

Negi, S.C., J.R.Ogilvie and J.C.Jofriet. 1987. Some mechanical and rheological properties of silages. *Canadian Agricultural Engineering*, 29(1): 59-64.

Peleg, M. and C.H.Mannheim. 1973. Effect of conditions on the flow properties of powdered sucrose. *Powder Technology*, 7(1): 45-50.

Peleg, M. 1977. Flowability of food powders and methods for its evaluation-a review. *Journal of Food Process and Engineering*, 1(4): 303-328.

Peleg, M. and A.M.Hollenbach. 1984. Flow conditioners and anticaking agents. *Food Technology*, 38(3): 93-102.

Pilpel, N. 1965. Flow properties of non-cohesive powders. *Chemical and Process Engineering*, 46(4): 167-179.

Pilpel, N. 1970. Some effects of moisture on the flow and cohesiveness of powders. *Manufacturing Chemist & Aerosol News*, 41(4): 19-22.

Ploof, D.A. and J.W. arson. 1997. Measuring relative flowability of powders, *Ceramic Industry*, 147(1): 35-38.

Ramanan, P., P.S.Rao, S.C.Babu and B.Pitchumani. 1981. The effect of size distribution and fines on the flow properties of raw mix in cement plant. *Bulk Solids Handling: the International Journal of Storing and Handling Bulk Materials*, 17(2): 253-256.

Schonlebe, K. 1991. Flow behaviour of binary coal mixtures. *Aufbereitungstechnik*, 32: 335-343.

Schulze, D. 1996a. Measuring powder flowability: a comparison of test methods Part I. *Powder and Bulk Engineering*, 10(4): 45-61.

Schulze, D. 1996b. Measuring powder flowability: a comparison of test methods Part II. *Powder and Bulk Engineering*, 10(6): 17-28.

Schulze, D. 1996c. Flowability and time consolidation measurements using a ring shear

tester. *Powder Handling and Processing*, 8(30): 221-226.

Stainforth, P.T. and R.E.R.Berey. 1973. A general flowability index for powders. *Powder Technology*, 8:243-251.

Stewart, B.R. 1968. Effect of moisture content and specific weight on internal friction properties of sorghum grain. *Transactions. of the ASAE*, 11(2): 260-266.

Svarovsky, L. 1987. Powder Testing Guide: *Methods of Measuring the Physical Properties of Bulk Powders*, 72-78. New York: Elsevier Applied Science.

Teunou, E., J.J.Fitzpatrick, and E. C. Synnott. 1999. Characterization of food powder flowability. *Journal of Food Engineering*, 39 (1): 31-37.

Teunou, E. and J.J.Fitzpatrick. 1999. Effect of relative humidity and temperature on food powder flowability. *Journal of Food Engineering*, 42 (2): 109-116.

Train, D. 1958. Some aspects of the property of angle of repose of powders *J. Pharm. Pharmacolgy*. 10:127T-135T.

Tsunakawa, H. 1982. Measurements of the failure properties of granular materials and cohesive powders. *Powder Technology*, 33(2): 249-256.

Williams, J.C., A.H. Birks, D. Bhattacharya. 1971. The direct measurement of the failure function of a cohesive powder. *Powder Technology*, 4(1): 328-337.

Williams, J.C. 1990. The storage and flow of powders. In M. Rhodes (Ed.). *Principles of Powder Technology* (pp. 91-118). Chichester: John Wiley & Sons Ltd.

Appendix A.1

Regression Analysis

1) The regression equation with only main effects.

The regression equation for angle of internal friction is:

$$\text{angle} = 47.983 + 0.078 \text{ particle size} - 0.124 \text{ moisture} + 1.324 \text{ flow enhancer}$$

Where particle size has units of mm, moisture content corresponding to equilibrium RH in units of %RH, flow enhancer has units of %.

Condition indices

1	2	3	4
1.000	2.708	3.721	10.750

Variance proportions

	1	2	3	4
CONSTANT	0.004	0.002	0.031	0.962
SIZE	0.024	0.163	0.777	0.036
MOISTURE	0.005	0.003	0.061	0.931
ENHANCER	0.030	0.825	0.127	0.017

Dep Var: ANGLE N: 24 Multiple R: 0.634 Squared multiple R: 0.402

Adjusted squared multiple R: 0.312 Standard error of estimate: 3.650

Effect	Coefficient	Std Error	Std Coef	Tolerance	t	P(2 Tail)
CONSTANT	47.983	3.329	0.000	.	14.414	0.000
SIZE	0.078	0.298	0.045	1.000	0.261	0.797
MOISTURE	-0.124	0.050	-0.433	1.000	-2.504	0.021
ENHANCER	1.324	0.497	0.461	1.000	2.666	0.015

Effect	Coefficient	Lower	< 95%>	Upper
CONSTANT	47.983	41.039		54.927
SIZE	0.078	-0.544		0.699
MOISTURE	-0.124	-0.228		-0.021
ENHANCER	1.324	0.288		2.361

Correlation matrix of regression coefficients

	CONSTANT	SIZE	MOISTURE	ENHANCER
CONSTANT	1.000			
SIZE	-0.313	1.000		
MOISTURE	-0.895	0.000	1.000	
ENHANCER	-0.224	0.000	0.000	1.000

Analysis of Variance

Source	Sum-of-Squares	df	Mean-Square	F-ratio	P
Regression	179.181	3	59.727	4.482	0.015
Residual	266.490	20	13.324		

The regression equation for cohesion is:

cohesion = 4.777 + 0.086 particle size - 0.052 moisture + 0.16 flow enhancer

Condition indices

1	2	3	4
1.000	2.708	3.721	10.750

Variance proportions

	1	2	3	4
CONSTANT	0.004	0.002	0.031	0.962
SIZE	0.024	0.163	0.777	0.036
MOISTURE	0.005	0.003	0.061	0.931
ENHANCER	0.030	0.825	0.127	0.017

Dep Var: COHESION N: 24 Multiple R: 0.834 Squared multiple R: 0.696

Adjusted squared multiple R: 0.650 Standard error of estimate: 0.612

Effect	Coefficient	Std Error	Std Coef Tolerance	t	P(2 Tail)
CONSTANT	4.777	0.558	0.000	8.553	0.000
SIZE	0.086	0.050	0.212	1.722	0.101
MOISTURE	-0.052	0.008	-0.771	-6.256	0.000
ENHANCER	0.160	0.083	0.237	1.920	0.069

Effect	Coefficient	Lower	< 95%>	Upper
CONSTANT	4.777	3.612		5.942
SIZE	0.086	-0.018		0.190
MOISTURE	-0.052	-0.070		-0.035
ENHANCER	0.160	-0.014		0.334

Correlation matrix of regression coefficients

	CONSTANT	SIZE	MOISTURE	ENHANCER
CONSTANT	1.000			
SIZE	-0.313	1.000		
MOISTURE	-0.895	0.000	1.000	
ENHANCER	-0.224	0.000	0.000	1.000

Analysis of Variance

Source	Sum-of-Squares	df	Mean-Square	F-ratio	P
Regression	17.172	3	5.724	15.262	0.000
Residual	7.501	20	0.375		

2) The regression equation with main effect and two – way interaction.

The regression equation for angle of internal friction is:

$$\text{Angle} = 28.412 + 4.625 \text{ particle size} + 0.204 \text{ moisture} + 3.628 \text{ flow enhancer} - 0.076 \text{ moisture*particle size} + 0.023 \text{ enhancer*particle size} - 0.041 \text{ enhancer*moisture}.$$

Condition indices

1	2	3	4	5
1.000	2.401	3.239	7.303	9.325
6	7			
20.343	33.737			

Variance proportions

	1	2	3	4	5
CONSTANT	0.000	0.001	0.005	0.031	0.016
SIZE	0.001	0.003	0.004	0.001	0.076
MOISTURE	0.000	0.001	0.006	0.001	0.065
ENHANCER	0.001	0.007	0.001	0.001	0.096
MOISTURE	0.001	0.003	0.004	0.044	0.014
ENHANCER	0.004	0.019	0.110	0.527	0.317
ENHANCER	0.001	0.007	0.002	0.067	0.013

	6	7
CONSTANT	0.014	0.933
SIZE	0.235	0.681
MOISTURE	0.011	0.915
ENHANCER	0.669	0.226
MOISTURE	0.268	0.666
ENHANCER	0.005	0.018
ENHANCER	0.702	0.208

Dep Var: ANGLE N: 24 Multiple R: 0.943 Squared multiple R: 0.889

Adjusted squared multiple R: 0.850 Standard error of estimate: 1.706

Effect	Coefficient	Std Error	Std Coef	Tolerance	t	P(2 Tail)
CONSTANT	28.412	2.899	0.000	.	9.801	0.000
SIZE	4.625	0.591	2.683	0.056	7.825	0.000
MOISTURE	0.204	0.046	0.709	0.253	4.411	0.000
ENHANCER	3.682	1.011	1.282	0.053	3.642	0.002
MOISTURE						
*SIZE	-0.076	0.009	-2.893	0.053	-8.222	0.000
ENHANCER						
*SIZE	0.023	0.093	0.040	0.253	0.246	0.808
ENHANCER						
*MOISTURE	-0.041	0.015	-0.900	0.056	-2.625	0.018

Effect	Coefficient	Lower	< 95%>	Upper
CONSTANT	28.412	22.296		34.528
SIZE	4.625	3.378		5.872
MOISTURE	0.204	0.106		0.301
ENHANCER	3.682	1.549		5.815
MOISTURE				
*SIZE	-0.076	-0.096		-0.057
ENHANCER				
*SIZE	0.023	-0.173		0.219
ENHANCER				
*MOISTURE	-0.041	-0.073		-0.008

Correlation matrix of regression coefficients

	CONSTANT	SIZE	MOISTURE	ENHANCER	MOISTURE
CONSTANT	1.000				
SIZE	-0.714	1.000			
MOISTURE	-0.956	0.663	1.000		
ENHANCER	-0.523	0.076	0.462	1.000	
MOISTURE	0.673	-0.943	-0.704	0.000	1.000
ENHANCER	0.168	-0.236	0.000	-0.322	0.000
ENHANCER	0.481	0.000	-0.503	-0.919	0.000
	ENHANCER	ENHANCER			
ENHANCER	1.000				
ENHANCER	0.000	1.000			

Analysis of Variance

Source	Sum-of-Squares	df	Mean-Square	F-ratio	P
Regression	396.183	6	66.031	22.683	0.000
Residual	49.488	17	2.911		

The regression equation for cohesion is:

$$\text{cohesion} = 2.354 + 0.669 \text{ particle size} - 0.007 \text{ moisture} + 0.221 \text{ flow enhancer} - 0.011 \text{ moisture*particle size} + 0.055 \text{ enhancer*particle size} - 0.004 \text{ enhancer*moisture}.$$

Condition indices

1	2	3	4	5
1.000	2.401	3.239	7.303	9.325
6	7			
20.343	33.737			

Variance proportions

	1	2	3	4	5
CONSTANT	0.000	0.001	0.005	0.031	0.016
SIZE	0.001	0.003	0.004	0.001	0.076
MOISTURE	0.000	0.001	0.006	0.001	0.065
ENHANCER	0.001	0.007	0.001	0.001	0.096
MOISTURE	0.001	0.003	0.004	0.044	0.014
ENHANCER	0.004	0.019	0.110	0.527	0.317
ENHANCER	0.001	0.007	0.002	0.067	0.013

	6	7
CONSTANT	0.014	0.933
SIZE	0.235	0.681
MOISTURE	0.011	0.915
ENHANCER	0.669	0.226
MOISTURE	0.268	0.666
ENHANCER	0.005	0.018
ENHANCER	0.702	0.208

Dep Var: COHESION N: 24 Multiple R: 0.957 Squared multiple R: 0.915

Adjusted squared multiple R: 0.885 Standard error of estimate: 0.351

Effect	Coefficient	Std Error	Std Coef	Tolerance	t	P(2 Tail)
CONSTANT	2.354	0.596	0.000	.	3.949	0.001
SIZE	0.669	0.122	1.650	0.056	5.506	0.000
MOISTURE	-0.007	0.010	-0.102	0.253	-0.729	0.476
ENHANCER	0.221	0.208	0.327	0.053	1.063	0.303
MOISTURE						
*SIZE	-0.011	0.002	-1.788	0.053	-5.813	0.000
ENHANCER						
*SIZE	0.055	0.019	0.407	0.253	2.893	0.010
ENHANCER						
*MOISTURE	-0.004	0.003	-0.399	0.056	-1.332	0.201

Effect	Coefficient	Lower	< 95%>	Upper
CONSTANT	2.354	1.096		3.612
SIZE	0.669	0.413		0.926
MOISTURE	-0.007	-0.027		0.013
ENHANCER	0.221	-0.218		0.660
MOISTURE				
*SIZE	-0.011	-0.015		-0.007
ENHANCER				
*SIZE	0.055	0.015		0.096
ENHANCER				
*MOISTURE	-0.004	-0.011		0.002

Correlation matrix of regression coefficients

	CONSTANT	SIZE	MOISTURE	ENHANCER	MOISTURE
CONSTANT	1.000				
SIZE	-0.714	1.000			
MOISTURE	-0.956	0.663	1.000		
ENHANCER	-0.523	0.076	0.462	1.000	
MOISTURE	0.673	-0.943	-0.704	0.000	1.000
ENHANCER	0.168	-0.236	0.000	-0.322	0.000
ENHANCER	0.481	0.000	-0.503	-0.919	0.000

	ENHANCER	ENHANCER
ENHANCER	1.000	
ENHANCER	0.000	1.000

Analysis of Variance

Source	Sum-of-Squares	df	Mean-Square	F-ratio	P
Regression	22.580	6	3.763	30.569	0.000
Residual	2.093	17	0.123		

Appendix A.2

Particle Size Analysis

1) Average particle size of two 25g samples ground through 6-mm screen in the Wiley laboratory mill.

Sieve #	Sieve size (micron)	Sample 1 (g)	Sample 2 (g)	Average (g)	% retained	Factor	Product
14	1400	1.62	1.95	1.79	7.22	6.00	43.33
18	1000	3.50	3.75	3.62	14.63	5.00	73.14
25	710	4.71	5.10	4.91	19.81	4.00	79.23
35	500	4.86	4.96	4.91	19.82	3.00	59.46
45	355	4.37	4.47	4.42	17.84	2.00	35.67
60	250	2.87	2.57	2.72	10.98	1.00	10.98
Pan		2.61	2.20	2.40	9.70	0.00	0.00
					100.00		301.81

$$\text{Fineness modulus} = \frac{301.809}{100} = 3.02$$

The average size of sample: $D = 0.0041 \times (2)^{3.02} = 0.033 \text{ inch} = 0.84 \text{ mm}$

2) Average particle size of two 25g samples ground through 1-mm screen in the Wiley laboratory mill.

Sieve #	Sieve size (micron)	Sample 1 (g)	Sample 2 (g)	Average (g)	% retained	Factor	Product
30	600	0.09	0.08	0.08	0.34	6.00	2.03
40	425	1.57	1.42	1.50	6.04	5.00	30.18
45	355	3.04	2.93	2.99	12.06	4.00	48.23
50	300	4.09	3.94	4.02	16.21	3.00	48.63
60	250	4.39	4.35	4.37	17.63	2.00	35.27
70	212	3.22	3.23	3.23	13.03	1.00	13.03
Pan		8.33	8.74	8.54	34.47	0.00	0.00
					100.00		177.38

$$\text{Fineness modulus} = \frac{177.38}{100} = 1.78$$

The average size of sample: $D = 0.0041 \times (2)^{1.78} = 0.014 \text{ inch} = 0.36 \text{ mm}$

2

VITA

Yu Zou

Candidate for the Degree of

Master of Science

Thesis: ANGLE OF INTERNAL FRICTION AND COHESION OF CONSOLIDATED
GROUND MARIGOLD PETALS AS A FUNCTION OF PARTICLE SIZE,
MOISTURE CONTENT, AND FLOW ENHANCER.

Major Field: Biosystems Engineering

Biographical:

Personal Data: Born in Hezhou, Guangxi, China, on February 19, 1972, the
daughter of Dingzong Zhou and Peixian Liang.

Education: Graduated from Hezhou High School, Hezhou, Guangxi, China in July
1989; received Bachelor of Science degree in Sugar Engineering from
South China University of Technology, Guangzhou, China in July 1993.
Completed the requirements for the Master of Science degree with a major
in Biosystems Engineering at Oklahoma State University in July 2000.

Experience: Employed by Oklahoma State University, Biosystems and
Agricultural Engineering Department as a Graduate Research Assistant,
1998 to present; employed by Pepsi-Asia Beverage Company, Guangzhou,
China, as a Production Line Supervisor, 1996 to 1998; employed by
Huihua Animal Health Products Company, Guangzhou, China, as a
technologist, 1993 to 1996.

Professional Memberships: Institute of Food Technologists.